Intranasal treatment with a novel immunomodulator mediates innate immune protection against lethal Pneumonia Virus of Mice.

A Thesis Submitted to the College of
Graduate Studies and Research
In Partial Fulfillment of the Requirements
For the Degree of Master of Science
In the Department of Microbiology and Immunology
University of Saskatchewan
Saskatoon, Canada

By

ELISA CATALINA MARTINEZ PEÑA

PERMISSION TO USE

In presenting this thesis in partial fulfillment of the requirements for a Postgraduate degree from the University of Saskatchewan, I agree that the Libraries of this University may make it freely available for inspection. I further agree that permission for copying of this thesis in any manner, in whole or in part, for scholarly purposes may be granted by the professor who supervised my thesis work or, in their absence, by the Head of the Department or the Dean of the College in which my thesis work was done. It is understood that any copying or publication or use of this thesis or parts thereof for financial gain shall not be allowed without my written permission. It is also understood that due recognition shall be given to me and to the University of Saskatchewan in any scholarly use which may be made of any material in my thesis.

Request for permission to copy or make other use of material in this thesis in whole or part should be addressed to:

Head of the Department of Microbiology and Immunology
2D01, Health Sciences Building
107 Wiggins Road
University of Saskatchewan
Saskatoon, Saskatchewan, S7N 5E5
Canada

ABSTRACT

Respiratory syncytial virus (RSV) is the major causative agent of acute lower respiratory tract infections in infants and young children. Unfortunately, there are no licensed RSV vaccines available, and the few treatment options for high-risk individuals are either extremely costly or cause severe side effects and toxicity. Thus, the development of effective vaccines and therapeutic interventions against RSV is a preeminent public health priority.

Pneumonia virus of mice (PVM) causes similar clinical symptoms and disease in mice to those observed in RSV-infected patients, and therefore is used as a model for pathogenesis studies. Lethal PVM infection (i.e. 3000 pfu) in Balb/c mice is characterized by 20% weight loss in total body weight, rough coats, abnormal posture, nasal discharge, and difficulty breathing due to neutrophilia, edema and alveolitis in the lower airways. Also, these mice will succumb to the infection between days 6 and 7 p.i.

Immunomodulation mediated by a novel formulation composed of the toll-like receptor 3 agonist poly I:C, an innate defense regulator peptide and a polyphosphazene (i.e. P-I-P) was first assessed in healthy adult Balb/c mice. Subsequently, the protective potential of P-I-P was further investigated in the context of a lethal PVM infection. P-I-P induced highest mRNA and protein expression of chemokines and cytokines in the lung milieu between 6 and 24 hr post-treatment. In addition, a single dose of P-I-P protected adult mice against PVM when given 24 hr prior to challenge. These animals displayed minimal body weight changes, no clinical disease, 100% survival, as well as reduced lung virus titers and pathology. P-I-P pre-treatment induced early mRNA and protein expression of key chemokine and cytokines, and decreased neutrophil and eosinophil numbers in the lungs, resulting in an overall modulation of the delayed exacerbated nature of PVM disease without short-term side effects. It was determined that the protective effects of P-I-P prophylaxis were maintained if administered up to 3 days prior to lethal PVM infection. On day 14 post-infection, P-I-P-treated survivor mice were confirmed to be PVM-free. These results demonstrate the capacity of this formulation to prevent PVM and possibly other viral respiratory infections.

ACKNOWLEDGEMENTS

First and foremost, I would like to kindly thank my supervisor, Dr. Sylvia van den Hurk, for giving me the wonderful opportunity to work in her laboratory since I was a young summer student. No words can express how thankful I am for her mentorship and continued support during the past four years of my academic journey. Also, my deepest gratitude goes to my advisory committee members: Dr. Calliope Havele, Dr. Harold Bull and Dr. Wei Xiao for their guidance, suggestions and countless scientific discussions during our meetings.

I would like to acknowledge all the wonderful people of the A321 lab, as well as my colleagues from VIDO-InterVac, for both their scientific and moral support throughout the pursuit of my master's degree. I extend my sincere gratitude to Laura Latimer, for teaching me all the laboratory techniques and skills I needed to know to succeed during graduate school. I am also indebted to Dr. Ravendra Garg for his invaluable scientific input and guidance during my project, his expertise with flow cytometry, as well as our innumerable conversations about the interesting world of immunology. Thanks to Dr. Pratima Shrivastava for teaching me several PVM techniques and the basics of qPCR, and Dr. Susantha Gomis for all the help provided with the histopathology studies. In addition, I would like to express my profound appreciation to Sherry Tetland and all the VIDO-InterVac animal care staff, for being so careful and diligent with the handling of my mice, as well as their constant assistance during my experiments.

Last but certainly not least, I want to thank my family, close friends and loved ones for helping me endure the difficult times I experienced during this journey. Thank you Diego, for always believing in me when I no longer did. During rough times, you constantly encouraged me to look at the bright side. Without your boundless love and support, this wouldn't have been possible. Thank you mamita for giving the gift of life. Your endless love and unconditional support gave me the strength I needed to pursue my dreams through thick and thin. You are, and always will be my biggest inspiration. I am forever thankful to my grandparents, for being my biggest fans and never doubting that I was destined for greatness.

DEDICATION

This thesis is dedicated to the memory of my loving grandfather,

Daniel Arturo Peña Duran,

whose tenacity and hard work inspired me to become a better person every day.

Abuelito, eres y siempre seras mi héroe.

Te amo.

TABLE OF CONTENTS

LIST OF TABLES

LIST OF FIGURES

LIST OF ABBREVIATION

AAP	American Academy of Pediatrics
ALRIs	Acute lower respiratory infections
APC	Antigen presenting cell
BALF	Bronchoalveolar lavage fluid
BCC	Basal cell carcinoma
BCG	Bacillus Calmette–Guerin
BHK	Baby hamster kidney
BHV-1	Bovine herpesvirus 1
BRDC	Bovine Respiratory Disease Complex
BRSV	Bovine RSV
BVDV	Bovine Viral Diarrhea Virus
CAA	Chimpanzee Coryza Agent
CCL	Chemokine (C-C motif) ligand
CD	Cluster of differenciation
cDNA	Complementary DNA
COPD	Chronic obstructive pulmonary disease
CpG ODN	Cytosine-phosphate-guanosine oligodeoxynucleotides
CSF	Colony-stimulating factor
CXCL	Chemokine (C-X-C motif) ligand
DC	Dendritic cell
DNA	Deoxyribonucleic acid
ds	Double-stranded
ECP	Eosinophilic cationic protein
ECs	Epithelial cells
ELISA	Enzyme-linked immunosorbent assay
FACS	Fluorescence-activated cell sorting
FBS	Fetal bovine serum
FI-RSV	Formalin-inactivated RSV
GAPDH	Glyceraldehyde 3-phosphate dehydrogenase

GM-CSF	Granulocyte macrophage colony-stimulating factor
GPCRs	G protein-coupled receptors
H&E	Hematoxylin and eosin
HEp-2	Human epithelial type-2
HIV/AIDS	Human immunodecifiency virus and acquired immune deficiency syndrome
HPV	Human papilloma virus
hr	Hour
HSCT	Hematopoietic stem cell transplant
IDR	Innate defense regulator
IFN	Interferon
IFNAR	Interferon-α/β receptor
Ig	Immunoglobulin
IL	Interleukin
IP-10	Interferon gamma-inducible protein
IRF	Interferon-regulatory factor
IRS	Immunoregulatory sequence
ISG	Interferon-stimulated gene
IVIG	Intravenous immunoglobulin
JAK	Janus-activated kinase
KC	Keratinocyte chemoattractant
LPS	Lipopolysaccharides
LRT	Lower respiratory tract
M-CSF	Macrophage colony-stimulating factor
MCP-1	Monocyte chemotactic protein 1
MDA-5	Melanoma-differentiation-associated gene 5
min	Minute
MIP	Macrophage inflammatory protein
MOI	Multiplicity of infection
mRNA	Messenger RNA
NBF	Neutral buffered formalin
NF-κB	Nuclear factor-kappaB

NK	Natural Killer
NLRP	NACHT, LRR and PYD domains-containing protein
NLRs	Nucleotide-binding oligomerization domain-like receptors
NS	Nonstructural
P-I-P	Poly I:C-IDR peptide 1002-PCEP
p.i.	Post-infection
p.t.	Post-treatment
PAMPs	Pathogen-associated molecular patterns
PBMCs	Peripheral blood mononuclear cells
PBS	Phosphate-buffered saline
PCEP	Poly[di(sodiumcarboxylatoethylphenoxy)]phosphazene
PCR	Polymerase chain reaction
pDC	Plasmacytoid DC
pfu	Plaque-forming units
PIV	Parainfluenza virus
PMNs	Polymorphonuclear leukocytes
Poly I:C	Polyinosinic-polycytidylic acid
PRRs	Pattern recognition receptors
PVM	Pneumonia Virus of Mice
qPCR	Quantitative real-time PCR
RANTES	Regulated on activation, normal T cell expressed and secreted
RIG-I	Retinoic acid-inducible gene I
RLRs	Retinoic acid-inducible gene-I-like receptors
RNA	Ribonucleic acid
ROS	Reactive oxygen species
RSV	Respiratory Syncytial Virus
SARS-CoV	Severe Acute Respiratory Syndrome coronavirus
Sec	Second
SH	Small hydrophobic
SLE	Systemic lupus erythematosus
SPAG-2	Small particle aerosol generator model-2

SQSTM1	Sequestosome-1
STAT	Signal transducer and activator of transcription
TGF	Transforming growth factor
Th1	T helper cell type 1
Th2	T helper cell type 2
TLRs	Toll-like receptors
TNF	Tumor necrosis factor
TRAF	TNF receptor-associated factor
Treg	Regulatory T cell
URT	Upper respiratory tract

1. INTRODUCTION AND LITERATURE REVIEW

1.1 Respiratory Syncytial Virus: Disease burden and epidemiology.

Respiratory syncytial virus (RSV) is an enveloped, negative-sense single-stranded RNA virus, genus *Pneumovirus* of the *Paramyxoviridae* family. RSV disease was first documented in 1956, when an outbreak of severe coryza illness was reported in a colony of chimpanzees [1, 2]. The recovered agent responsible for the clinical symptoms observed in these animals was initially called "chimpanzee coryza agent" (CAA). Shortly after, the same virus was isolated from respiratory secretions of infants and young children with bronchiolitis and pneumonia [2, 3]. It was suggested that CAA was a virus of human origin, which could have been transmitted by the laboratory personnel in charge of handling the chimpanzees. In 1957, CAA was renamed "respiratory syncytial virus" as this agent had tissue tropism for cells of the respiratory tract and infection of the airway epithelium lead to syncytia formation [4].

Since its discovery in the mid-1950s, RSV is considered the most common cause of bronchiolitis and pneumonia in infants and young children. Global RSV disease accounts for approximately 34 million infections and 175,000 deaths each year [1, 5]. RSV exists as a single serotype with two major antigenic groups, namely A and B. During yearly epidemics, it has been observed that both subtypes tend to co-circulate within a given season. However, one of either genotype usually predominates [6, 7]. RSV-A and B subtypes mostly differ in sequences and epitopes of the attachment glycoprotein [1, 6]. It is thought that these antigenic variances might contribute to differences in infection and

disease susceptibility [7]. Several groups demonstrated that group A RSV was associated with worsened symptoms and enhanced clinical severity than those caused by the RSV-B subtype [1, 7]. However, some studies yielded controversial results suggesting that either subgroup was equally as pathogenic as the other. Thus, it remains unclear whether RSV strain differences play a role in disease severity [1, 7]. RSV circulates year-round within communities. In temperate regions, outbreaks are routinely reported during the fall, winter, and spring months, while in tropical climates highest incidence occurs during the rainy season [1, 6, 8]. Virus transmission occurs most commonly through direct contact with infected individuals and their secretions, via large particle droplets and/or fomites [1, 9]. Due to the extremely infectious nature of the virus, it is estimated that most children become infected with RSV by the age of two [1, 6]. Reinfections can occur repeatedly throughout life, often with mild upper respiratory tract (URT) symptoms in most healthy older children and adults [9-11]. Pre-term babies, newborn infants between 2 and 4 months of age, immunocompromised individuals, and the elderly are at highest risk of developing severe RSV disease [9, 12]. In these populations, the virus can infect the lower respiratory tract (LRT), often leading to hospitalizations and in worst cases death [13].

In the USA, the average RSV hospitalization rate for infants is estimated to be 26 per 1,000, and for children between the ages of 1 to 5 is 1.8 per 1,000 [14]. Similar numbers were also reported in other developed nations, with highest hospitalization rates among infants and young children less than 5 years of age [15, 16]. In contrast to influenza- and parainfluenza virus (PIV)-induced hospitalization, RSV was responsible for 3 times higher rates among children, and 6 to 8 times greater in infants [1]. RSV-associated

mortality is rare in developed countries. In the USA, it is estimated that no more than 500 fatal cases occur each year [17]. Death related to RSV infections during the winter season in the Netherlands is usually not observed among patients 1 to 18 years old [18]. Elderly patients are also at an increased risk of developing severe RSV disease, with hospitalization rates ranging from 14,000 to 62,000 per year in the USA [19]. Underlying conditions such as congestive heart failure and chronic lung disease are major contributing factors for high rates of hospitalization among the elderly [1]. In this population, RSV infections were responsible for 10.6% of hospitalizations for pneumonia, 11.4% for obstructive pulmonary disease, and 7.2% for asthma [20]. Mortality rates are also elevated in these patients. In the Netherlands, individuals 65 years of age and older have higher death rates during winter months than infants and young children [18].

There is a poor understanding of RSV burden in the developing world. Existing data denote that the virus accounts for a high incidence of acute lower respiratory infections (ALRIs) in young children and infants [21]. A study conducted in 2005 estimated that RSV-associated disease in developing nations occurred at greater than twice the rate as compared to developed countries. Furthermore, 99% of all RSV-related deaths were reported in these countries [1, 21]. Lower diagnostic potential, restricted access to healthcare, and high hospitalization costs are several factors limiting studies on RSV incidence in developing countries [21, 22]. Thus, available data describing RSV disease burden in these communities are likely to be an underestimate of the true nature of this infection [1, 21].

1.2 Treatments available against RSV disease.

Despite the significant public health burden of RSV in the world, there are no licensed vaccines available to date. In the 1960s, a vaccine candidate consisting of formalin-inactivated RSV (FI-RSV) in combination with alum was given intramuscularly to infants and young children [1, 5]. Unfortunately, this vaccine failed at inducing protective immune responses in these populations. Instead, subjects were primed to develop exacerbated disease upon exposure to subsequent natural RSV infections [1]. Also, FI-RSV vaccinated individuals displayed higher rates of hospitalizations and deaths than control infants vaccinated with an inactivated PIV-3 vaccine [5, 9, 23]. The failure of this vaccine candidate was mainly attributed to the generation of strong Th2-biased responses, high influx of lymphocytes, eosinophils, and neutrophils into the LRT, low avidity and non-neutralizing antibodies, poor toll-like receptor (TLR) activation, and minimal priming of $CD8^+$ cytotoxic T cells *in vivo* [5, 9, 10].

The management of patients with RSV bronchiolitis is primarily supportive in nature [11]. Treatment options consist of respiratory support with supplemental oxygen and mechanical ventilation, intravenous fluids, nasal suction, as well as the administration of bronchodilators and corticosteroids [1, 6]. Oxygen therapies are routinely used when oxygen saturation levels in the blood are below 90% [1]. Mechanical ventilators are often required when respiratory failure is observed, especially in high-risk patients such as infants and the immunocompromised [1]. The effectiveness of bronchodilator and corticosteroid treatments is controversial [1, 6, 24]. The latter therapy is often used when the lower airways are fully obstructed, resulting in difficulty breathing and wheezing.

There is evidence suggesting that administration of albuterol in patients with RSV-induced respiratory failure did not much improve lung function and disease outcome [25]. Similarly, several human trials lead to the conclusion that neither nebulized nor intravenous delivery of corticosteroids was effective at shortening the length of hospitalization among infants with RSV bronchiolitis [26].

1.2.1 Palivizumab

Several research groups conducting studies in cotton rats and humans demonstrated that passive transfer of immunoglobulins is a suitable approach to protect high-risk individuals from RSV disease [27]. It was found that convalescent sera from patients who previously had RSV did not contain sufficient RSV-specific neutralizing antibody levels to provide protection [27]. Thus, a high-titered intravenous immunoglobulin was created as a solution to this problem. RSV-IVIG (RespiGam; MedImmune, Inc., Gaithersburg, MD) was developed in 1996 as the first prophylactic agent against RSV infections in high-risk infants [1, 27]. This novel immunoglobulin consisted of pooled sera from individuals with high RSV-specific neutralizing antibody titers [1]. It was shown that RSV-IVIG reduced the rates of RSV-associated LRTIs in high-risk infants and young children [28]. However, RSV-IVIG prophylaxis in infants with congenital heart disease was linked to fluid overload due to large infusion volumes, oxygen desaturation and fever [28]. Thus, the use of RSV-IVIG in this population is contraindicated [27]. As a result of the several disadvantages posed by this approach, a novel monoclonal anti-RSV neutralizing antibody was developed [29]. *Johnson et al*. described the effectiveness of

the MEDI-493 antibody, currently known as palivizumab, both *in vitro* and *in vivo* [29]. It was demonstrated that MEDI-493 successfully neutralizes RSV-A and -B infections in human epithelial type 2 (HEp-2) cells [27, 29]. In addition, MEDI-493 prophylaxis in cotton rats completely eliminated virus replication without interfering with the development of protective responses [27, 29].

Palivizumab (Synagis, MedImmune Vaccines, Inc., Gaithersburg, MD) is a humanized monoclonal antibody directed against the fusion (F) protein of RSV [1, 30]. In 1998, the US Food and Drug Administration (FDA) approved palivizumab to be used for the prophylaxis of high-risk infants and young children. This antibody is routinely administered as an intramuscular injection, and given as a single dose of 15 mg/kg every 30 days for a 5-month period [1, 6, 30]. Current guidelines recommend infants born at or before 32 weeks gestation, and currently age 6 or younger to receive palivizumab prophylactic therapy at the start of the local RSV season [1, 6, 30]. Two major human trials were conducted to assess the efficacy of palivizumab in high-risk pediatric patients [1]. It was concluded that the use of this antibody for prophylaxis was associated with a significant reduction in RSV-related hospitalization rates [31, 32]. Unlike RSV-IVIG, palivizumab did not cause any adverse effects in children with congenital heart disease [32].

Unfortunately, the extremely high cost and administration logistics of palivizumab limit its use to patients in the developing world [1, 9, 11]. Currently, the average cost of a 100 mg vial of palivizumab is $2,962 USD in the USA, and $1,505 CAD in Canada [33]. Several groups concluded that palivizumab prophylaxis in high-risk infants was not a cost-effective strategy to prevent RSV infections in this population [1, 34]. In addition,

patients must comply to follow a full course of palivizumab prophylaxis in order to reach sufficient levels of protective serum anti-RSV antibodies [1]. It is worth mentioning that palivizumab is certainly not a cure for RSV. According to several studies, palivizumab is most effective as a prophylactic agent, and not when used therapeutically [27]. This means that patients who already have an established RSV infection would not benefit from palivizumab therapy. While the use of palivizumab for prophylaxis has been successful at preventing RSV bronchiolitis in high-risk infants, it is still a non-sustainable approach to limit RSV infections and transmission within a community.

1.2.2 Ribavirin

Ribavirin (Virazole, Valeant Pharmaceuticals International, Aliso Viejo, CA), an FDA-approved broad-spectrum nucleoside analogue, is utilized to treat severe RSV bronchiolitis in high-risk infants and young children [1, 6, 24, 35]. It has been shown that ribavirin is also effective *in vitro* against measles virus, parainfluenza virus, adenovirus, hepatitis C virus and others [1, 35-37]. This antiviral drug does not affect the initial steps of a viral infection, such as attachment, penetration and uncoating [37]. Ribavirin acts primarily by inhibiting viral replication and transcription during the active growth phase [1, 36]. Nonetheless, its complete mechanism of action is yet to be elucidated.

Ribavirin is most commonly administered as an aerosolized formulation, but it can also be given through intravenous or oral routes [1]. The typical dose of this agent is 20 mg/ml, administered continuously for 12-18 hours over a period of 3-7 days [1, 35]. Ribavirin is usually delivered using a small particle aerosol generator model-2 (SPAG-2)

via a face mask inside an oxyhood or tent [35]. It has been demonstrated in several rodent models that ribavirin is a teratogenic substance [1, 24, 35, 37]. Therefore, this drug is contraindicated in pregnant women [1, 35]. Aerosolized ribavirin is also known to cause fatigue, nausea, headache, and anorexia [1]. In patients with chronic obstructive pulmonary disease (COPD) or asthma, ribavirin treatment has been correlated with an aggravation of respiratory function [1, 37]. Intravenous delivery of ribavirin is reserved for patients with poor lung penetration due to consolidative pneumonia [1]. On the other hand, oral ribavirin is much easier to administer but it has reduced bioavailability *in vivo* compared to aerosolized ribavirin [1]. Hemolytic anemia, nausea and leukopenia are several adverse effects associated with these two treatment routes [1, 37]. Ribavirin is also contraindicated in patients with a history of psychiatric disorders and severe depression as it can cause altered mental status [37].

Although ribavirin treatment is effective at limiting viral transcription both *in vitro* and *in vivo*, consistent evidence supporting a direct benefit of the drug at reducing hospitalization rates and ameliorating disease outcomes in patients with severe RSV bronchiolitis is lacking [1, 12, 24, 36]. It has been suggested that the presence or absence of live virions in the respiratory tract does not affect the severity and progression of RSV-induced inflammation [24]. *Ventre and Randolph* demonstrated that ribavirin therapy did not cause any significant improvement in mortality, length of hospitalization or ventilation in pediatric populations [38]. Thus, the American Academy of Pediatrics (AAP) does not recommend the routine use of this antiviral in such patients [1, 6]. Nevertheless, a combination of ribavirin and immunoglobulin (i.e. palivizumab) is commonly used in Hematopoietic Stem Cell Transplant (HSCT) recipients to treat RSV

bronchiolitis [35, 39]. Altogether, ribavirin treatment alone is not sufficient to treat RSV disease. Due to its high cost and all the potential side effects that can occur, this strategy is not the most suitable to implement in vulnerable populations like infants and young children.

1.3 Factors involved in pathogenesis of RSV infection.

RSV disease manifestations can range from mild rhinitis to severe bronchiolitis and pneumonia [1]. Primary RSV infections are characterized by high virus titers and delayed disease manifestations [40]. In individuals predisposed to enhanced RSV disease, a reduction in virus replication and rapid viral clearance is observed [40]. However, inflammatory responses tend to be exacerbated and often lead to immunopathology [40]. Certainly, clinical outcomes caused by RSV infections are multifactorial, which can be attributed to several host factors like genetics, age, premature birth, immunosuppression, underlying conditions, and others [1, 41]. RSV infections *in vivo* are mostly restricted to the superficial cells of the respiratory epithelium [1, 35, 42]. In the lower respiratory tract, RSV primarily targets ciliated cells of the small bronchioles and pneumocytes of the alveoli [42]. Severe RSV bronchiolitis shares similar pathology to influenza virus-, PIV-, and adenovirus-mediated bronchiolitis [40]. RSV replication in the LRT leads to edema by inducing necrosis of epithelial cells (ECs), high mucous production, and increased accumulation of leukocytes into the site of infection [35, 40, 42]. Thus, the small airways become obstructed resulting in patchy atelectasis and emphysema [35, 40]. Syncytia formation is not commonly observed *in vivo*, but is likely to occur in

immunocompromised patients [42]. A thorough understanding of the complex nature of RSV pathogenesis is pivotal for the development of successful vaccines and therapeutic interventions.

1.3.1 Innate Immune System.

The innate immune system acts as the first line of defense to ensure optimal pathogen control and survival of the host. In the context of RSV pathogenesis, the virus initiates its life cycle by primarily infecting the respiratory epithelium [1, 43, 44]. Resident macrophages of the lung milieu are also considered a major target for RSV infection within the tissue [41, 44, 45]. Following cellular attachment and entry, the virus and its pathogen-associated molecular patterns (PAMPs) are detected by several pattern recognition receptors (PRRs) located throughout the infected cell [1, 41, 43, 46]. Several PRRs involved in RSV pathogenesis are TLRs, nucleotide-binding oligomerization domain-like receptors (NLRs), and retinoic acid-inducible gene-I-like receptors (RLRs) [1, 41]. During replication, RSV is able to produce both single- and double-stranded RNA intermediates [47]. Out of all the PRRs present in the cell, TLRs have been the most studied in the context of RSV. For instance, TLR2, TLR3, TLR4 and TLR7 are known to be involved in the initial recognition of RSV by infected cells [1, 8]. As a result of this interaction, an array of signaling cascades are induced, leading to the production of both protective and pathological immune responses in the airways [1]. RSV infection activates the nuclear factor-kappaB (NF-κB) pathway, leading to the production of chemokine and cytokine proteins [40, 41, 47]. In addition, TLR signaling also leads to the

production of interferon (IFN-) α/β via IFN-regulatory factor 3 (IRF3) and IRF7 [40, 43, 46]. Similarly, RSV infection also leads to the rapid induction and increased expression of the retinoic acid-inducible gene I (RIG-I) in the cell cytoplasm [1, 48]. The engagement of this RLR with viral RNA results in the activation of NF-κB and IRF3, mediating the induction of both type I and type III IFNs [1, 49]. Several groups have demonstrated that RIG-I is indeed the major RLR contributing to the IFN response at the level of innate immunity [1, 48, 50].

It has been found that during RSV infection, ECs and macrophages produce high amounts of cytokines and chemokines including IL-8 (CXCL1/KC in mice), CXCL10 (IP-10), CCL2 (MCP-1), CCL3 (MIP-1α), CCL4 (MIP-1b), CCL5 (RANTES), IL-6, TNF-α, CXCL2 (MIP-2), and IL-1α/β [1, 40, 41, 51-54]. Similarly, elevated levels of such factors have been detected in respiratory secretions of hospitalized pediatric patients with RSV bronchiolitis [1, 51, 55]. The presence of these molecules within the lung milieu increases vascular permeability, leading to the selective recruitment and activation of different cell subsets into the tissue [8].

In the context of RSV infection, neutrophils, macrophages, eosinophils, and natural killer (NK) cells are the main innate immune cells involved in host defense and disease pathogenesis [1, 8, 41]. Neutrophils are the predominant innate immune cell present in the airways during severe RSV disease. According to a study of RSV bronchiolitis in pediatric patients, neutrophils constituted 93% of the cells in the URT and 76% in the LRT [8, 41, 51, 56]. Neutrophil chemotaxis is highly dependent on IL-8 [8]. It has been shown that nasal lavages of infants with RSV bronchiolitis contain high concentrations of IL-8 [41, 57]. Thus, the upregulation of this chemokine is associated

with RSV disease severity [8, 51]. While neutrophils are needed to mediate virus clearance at the level of the innate immune system, elevated neutrophil counts often promote RSV-induced immunopathology and tissue damage [41, 51]. This is explained by their ability to secrete chemokines and pro-inflammatory cytokines that could possibly amplify the existing inflammatory response in the airways [51]. Eosinophils have also been involved in severe RSV disease. In one study, higher concentrations of eosinophilic cationic protein (ECP) were found in nasopharyngeal secretions of children with RSV bronchiolitis [51, 58]. The research group concluded that eosinophil degranulation products might play a role in the development of severe RSV disease in the LRT [58]. Despite these findings, researchers failed to detect an increase in eosinophil numbers in pulmonary lavages of RSV-infected children [8, 41, 51, 58]. NK cells are innate immune cells that play a pivotal role in the control of viral infections. These cells possess high cytotoxic activity, and are mainly activated by IFN-β, IL-12 and TNF-α [8]. The exact contribution of NK cells to RSV pathogenesis is yet to be elucidated [8]. Nonetheless, NK cells are one of the earliest cells to infiltrate the lungs during RSV infections, and are responsible for most of the early IFN-γ production in the lung [8, 59]. *Weerd et al.* demonstrated that hospitalized children with RSV bronchiolitis had lower NK cell counts in the blood than control patients [60]. The group concluded that this decrease in cell numbers corresponded to increased recruitment of these peripheral cells into the respiratory tract [8, 60].

Viral infection of the airways results in the production of type I IFNs. These anti-viral molecules bind to the IFN-α/β receptor (IFNAR) on the cell surface, and signal through the Janus-activated kinase (JAK)/signal transducer and activator of transcription

(STAT) pathway [1, 43]. Subsequently, the nuclear translocation of a complex composed of STAT-1, STAT-2 and IFN regulatory factor 9 (IRF9) leads to the expression of several IFN-stimulated genes (ISGs) that contribute to the anti-viral response [43]. Interestingly, RSV has developed ways to counteract the host's innate immune responses. Nonstructural protein 1 (NS1) and 2 (NS2) of most paramyxoviruses are known to inhibit type I IFN production and signaling *in vivo* [1, 40]. These two proteins decrease STAT-2 signaling cascade by targeting this transcription factor for degradation [43, 61]. In addition, NS1 and NS2 proteins prevent type I IFN synthesis by blocking IRF3 and TNF receptor-associated factor 3 (TRAF3) signaling cascades [1, 62]. It has been demonstrated that STAT-1 and -2 knockout mice experience severe inflammation and increased Th2-type immune responses in the lungs during RSV infection [43, 63]. Thus, weakened type I IFN production and signaling might be a major factor contributing to severe RSV disease.

1.3.2 Adaptive Immune System.

While primary RSV infection successfully activates the host's adaptive immune system, protective immunity is often weak in nature and short-lived [1, 42]. This is consistent with the notion that humans experience multiple RSV reinfections throughout their lifetime. Nevertheless, the appropriate induction of adaptive immune responses has been shown to be a critical factor involved in optimal control of RSV disease in humans [41].

Regarding the humoral response following RSV infection in humans, there is an induction of both IgA in the URT and IgG antibodies in the serum [1, 41]. A long-lasting induction of secretory IgA is of importance as it confers protection to the URT [42]. This in turn can prevent the virus from reaching into the LRT of the individual and causing a more severe disease outcome. In contrast, serum IgG plays a major role in protecting the LRT as this antibody can access this compartment more readily than the URT [42]. Maternal neutralizing anti-RSV antibodies can cross the placenta during pregnancy and provide newborns and infants with a temporary means of protection against the virus earlier on in life [8, 42]. However, these immunoglobulins wane quite rapidly after infection [41]. There is evidence suggesting that most adults infected with RSV within 1 year of initial exposure experience a 4-fold decrease in neutralizing anti-RSV IgG titers [1]. Thus, the short-duration of the humoral response against RSV can explain why periodic reinfections tend to occur throughout life [1].

The role of cell-mediated immune responses in the context of RSV pathogenesis has been thoroughly investigated throughout the years. The nature of the T cell response following infection depends on the initial recognition of viral antigens by lung-resident dendritic cells (DCs) [41]. After engulfment of such antigens, cellular maturation occurs and DCs migrate into the lung draining lymph nodes where antigen presentation to naïve T cells takes place [1]. The nature of this event can have a major effect on the type of effector T cell response that is mounted against the virus. It has been concluded that T cell responses can mediate the effective clearance of the virus during primary infection [1]. Children with T cell immunodeficiencies experience longer periods of virus shedding and worsening of symptoms [1, 8]. According to a number of studies in mice, Th1

polarization of $CD4^+$ T cells is required for effective virus control and elimination [42]. The production and secretion of IFN-γ by these cells stimulates $CD8^+$ T cells to become cytotoxic and direct the specific destruction of RSV-infected cells [41-43]. In addition, IFN-γ can enhance phagocytic activity in macrophages leading to improved clearance of cellular debris within the tissue [43]. It was demonstrated that mice ablated from $CD8^+$ T cells prior to RSV infection display an overall delay in virus clearance [64]. Conversely, uncontrolled T-cell responses can also contribute significantly to exacerbating disease immunopathology [42]. Depletion of $CD4^+$ and $CD8^+$ T cells *in vivo* resulted in persistent virus replication with no remarkable signs of disease [64]. This supports the notion that the strength of the immune response to the virus, and not the virus itself, may enhance disease severity [8, 40]. The contribution of regulatory T cells (Tregs) to RSV disease pathogenesis has been recently studied. Treg depletion in mice prior to RSV infection resulted in increased disease severity that correlated with elevated levels of IL-6 and higher leukocyte recruitment into the airways [65]. It has been suggested that Tregs are important in limiting RSV-induced immunopathology, as their depletion did not have a major effect on virus clearance [66].

RSV-mediated pulmonary pathology is characterized by mucus overproduction and airway hyperreactivity [1]. It appears that $CD4^+$ T cells of the Th2 phenotype may be responsible for such clinical signs due to the secretion of Th2-type cytokines like IL-4, IL-5 and IL-13 [1]. Additional reasons supporting the role of these cells in RSV pathogenesis include the general tendency of the neonatal immune system to mount Th2-biased responses, and the similarities between RSV-induced pathological lesions and the asthma phenotype (i.e. high IgG1 and IgE antibody titers, eosinophil accumulation and

degranulation in the lower airways) [40, 42]. It has been reported that there is a strong association between elevated mRNA expression and protein concentration of Th2 cytokines in nasal secretions and stimulated peripheral blood mononuclear cells (PBMCs) and disease severity in pediatric patients [42]. While RSV infection in humans is able to induce both Th1 and Th2 responses, disease severity is highly dependent on host factors that are likely to affect the overall balance of the immune response. Ultimately, a better understanding on how age and host's genetics can shape RSV disease is needed in order to fully comprehend the complex nature of the virus.

1.4 Pneumoviruses as animal models of RSV disease.

Despite numerous attempts to fully understand the nature of RSV pathogenesis in humans, research involving subjects of different age groups and varying degrees of disease susceptibility is often limited by a number of factors. RSV infections in healthy individuals are usually self-limited and do not require hospitalization [51]. Thus, only the most severe manifestations of RSV disease can be studied in detail as the milder forms often go unreported [51]. Additionally, most studies are based on samples obtained from non-invasive procedures (i.e. PBMCs, nasal washes, lung aspirates, etc.) as there is limited accessibility to the LRT of infected individuals [51]. Needless to say, the numerous ethical concerns surrounding RSV studies in the LRT of healthy volunteers pose an even greater challenge in the study of the RSV disease spectrum [1]. One way to overcome such hindrances is to use appropriate animal models. These models provide a more dynamic and flexible setting to test hypotheses *in vivo,* addressing some of those

inquiries regarding the mechanism of disease pathogenesis. Ultimately, animal models are necessary tools to assess the safety and efficacy of novel vaccines and therapeutics during preclinical trials [67].

Currently, human RSV disease can be studied in the laboratory by the use of two major types of animal modeling. Heterologous host-virus models involve the infection of semi-permissive animals like chimpanzees, sheep, cotton rats and mice with human RSV [6, 67]. On the other hand, cognate host-virus models are based on other pneumoviruses infecting their natural hosts. Examples of the latter include bovine RSV (BRSV) and pneumonia virus of mice (PVM) [6, 67]. While there are unique advantages and disadvantages to each individual animal model, it is important to realize that not a single experimental system in isolation can be used to answer all the questions regarding the human RSV disease spectrum. Besides, the main hypothesis and specific objectives of one's research should dictate what the most appropriate disease model is for use in the laboratory.

1.4.1 Heterologous host-virus models.

1.4.1.1 Chimpanzee

It has been documented that young chimpanzees (i.e. 15-18 month old) are highly permissible to the virus, usually leading to productive infections [68]. Most animals exhibit URT disease symptoms like rhinorrhea, sneezing and coughing after primary RSV infection [67, 69, 70]. Unfortunately, a number of researchers have reported that

chimpanzees experimentally infected with RSV do not show signs or symptoms of LRT disease [67, 70]. The high genetic and anatomical similarities between chimpanzees and humans are major advantages of this model [67, 69]. However, high cost, limited accessibility, and the numerous ethical constrains of working with such animals restricts the use of this model for RSV pathogenesis studies [67, 68, 70]. Currently, the chimpanzee model is primarily used for the evaluation of novel vaccine candidates [67, 68].

1.4.1.2 Sheep

Recently, the use of a newborn lamb model has been proposed to be more suitable for RSV pathogenesis studies *in vivo* [51, 67]. Disease outcomes of experimentally infected neonatal lambs resemble closely the pathology observed in infants with RSV bronchiolitis [51]. Unlike the chimpanzee model, there is evidence of both upper and lower respiratory tract disease in newborn (2-3 days old) lambs infected with RSV [51, 67]. These animals presented with fever, coughing, bronchiolitis resulting from entrapment of cellular debris, mild interstitial pneumonia, and a prominent infiltration of neutrophils, macrophages and effector lymphocytes in the lungs [67]. In addition, high concentrations of IL-8 and TNF-α were detected in the lungs of these lambs and virus replication in the airways was robust [67]. Importantly, the respiratory tract of sheep and humans share a similar anatomical structure [51]. Unlike rodents, alveolar development in both species starts preterm [51]. Despite the fact that the availability of reagents and

molecular tools to analyze sheep samples has greatly increased over the years, it still remains a big disadvantage of this animal model for RSV research purposes [67].

1.4.1.3 Cotton rat

Over the past few decades, the cotton rat *Sigmodon hispidus* has become widely utilized for the study of RSV pathogenesis [1, 67]. In addition to being susceptible to RSV, these animals can support the replication of other human respiratory pathogens like influenza virus, PIV, and metapneumovirus [1]. Unlike most rodents, cotton rats are highly permissive to RSV and infections can be established throughout life [1, 69]. Thus, this model has been used to further study the differences in RSV disease susceptibility that occur in infants, elderly, and immunosuppressed populations [1]. In 1971, *Dreĭzin et al.* were the first group to describe the experimental infection of RSV in cotton rats [71]. Since then, it has been demonstrated that these animals are approximately 100-fold more permissive to RSV than inbred laboratory mice [1, 67, 69]. While RSV-infected cotton rats do not show major clinical symptoms like nasal discharge and changes in weight, in terms of histopathological lesions, these animals display mild signs of bronchiolitis and pneumonia following RSV infection [1, 67]. There is evidence that both the upper and lower respiratory tract can become infected with RSV [67]. However, virus replication lasts longer in the nose than in the lungs [1]. Following RSV infection, the inflammatory response is characterized by lymphocyte infiltration into the airways and increased levels of CCL3, CCL2 and IFN-γ in the site of infection [67]. Importantly, cotton rats have served as a surrogate model used to recapitulate the FI-RSV-enhanced disease previously

reported in human subjects. Thus, this model has become an indispensable tool to assess the safety of vaccines, antivirals and immunotherapeutics in preclinical studies [1, 67, 69]. Nevertheless, there are several drawbacks that might limit the use of such animal model system. For instance, RSV-infected cotton rats do not present with overt signs of disease [1]. Additionally, these small animals are difficult to handle, reagent availability is limited, and transgenic or knockout strains have yet to be developed [1, 67].

1.4.1.4 Mice

Initially described in 1979 by *Prince et al.*, the inbred laboratory mouse model has become quite popular over the years as a means to study experimental human RSV disease *in vivo* [6, 67, 72]. Most wild-type inbred mice are considered semi-permissive hosts for RSV [67]. Virus replication is limited, and even in the most susceptible strains, such as Balb/c, a high virus inoculum is required to obtain a productive infection [67, 70]. Clinical signs are moderate and are usually restricted to changes in total body weight, reduced mobility and rough coats [67]. As a result, different RSV strains (e.g. A/long) and human clinical isolates (Line 19, RSV 2-20) can be used to mimic a more severe disease presentation in mice [67]. Overall, the bronchoalveolar lavage fluid (BALF) of Balb/c mice infected with a high dose of RSV show elevated levels of TNF-α, IL-6, IFN-γ, CCL3, CCL5, and CXCL1 [67]. Effector lymphocytes are the most prominent cell type infiltrating the lungs following infection in this animal model [67]. Histopathological lesions include perivasculitis and peribronchiolitis, and in some cases, interstitial pneumonia is observed [67, 68]. In terms of age, experimentally infected neonatal Balb/c

mice develop asthma-like symptoms such as airway hyperreactivity, mucus overproduction, eosinophilia and a distinct Th2-biased response [51, 67, 73]. In contrast, RSV infection in adult Balb/c mice induces a Th1-biased response, with high concentrations of IFN-γ in both lung and BALF [68, 73]. A clear downside of using this animal model is the numerous differences between innate and adaptive immune responses of humans and mice [67]. Additionally, pneumoviruses are known to be species-specific, thus studies in cognate hosts are better suited to obtain an understanding of fundamental immune-mediated mechanisms of severe infection [13]. Other limitations in using rodents as animal models include the distinct neutrophil and lymphocyte ratios in blood, and differences in lung anatomy [13, 67, 69]. Nonetheless, the RSV mouse model has major advantages, such as the vast availability of reagents, immunological tools, knockout and transgenic strains, cost-effectiveness and ease of housing and handling [6, 67, 70].

1.4.2 Cognate host-virus models.

1.4.2.1 Mice and Pneumonia Virus of Mice (PVM)

Better animal models to study RSV pathogenesis can arise from the use of other pneumoviruses matched to their cognate hosts. In turn, this may provide us with a more accurate representation of natural infection and disease [1]. In the last thirty years, the pneumonia virus of mice (PVM) has been considered as a mouse model of natural RSV disease [13, 51]. PVM is closely related to RSV, both belonging to the same viral family

and subfamily, and inducing similar disorders in their natural hosts [74]. Unlike RSV infection in mice, PVM replicates in the lower airways to extremely high titers in response to as little as 10 plaque-forming units (pfu) of virus inoculum [12, 13, 51, 69]. In addition, PVM infections can lead to high mortality rates in susceptible mouse strains (e.g. 100% in Balb/c) [67]. However, a lower PVM inoculum dose or a more resistant mouse strain can change disease severity [67]. There are two fully characterized strains of PVM, PVMJ3666 and PVM-15. The genome sequence and organization of these strains is 99.7% identical to one another [13]. As both RSV and PVM are part of the same viral genus, they have very similar genomic structures and all PVM proteins have respective functional counterparts with RSV [13]. The virus has a preference for the bronchiolar epithelium, which mainly induces LRT disease symptoms such as tachypnea, airway obstruction and difficulty breathing [67]. Thus, it becomes very difficult to obtain URT disease presentation using the PVM infection model.

PVM-infected mice present with elevated levels of CCL2, CCL3, CCL5, CXCL1, TNF-α, IL-6, and IFN-γ in the lower airways. Neutrophils are the main cell population recruited into the LRT during active infection, playing a critical role in both PVM and RSV pathogenesis [13, 67, 68, 75]. As a result, histopathological lesions following PVM infection often result in peribronchiolitis with progression to edema, alveolitis, and hemorrhage [67]. Similar to RSV in humans, age is considered a major determinant in PVM-mediated clinical disease [67, 76]. Unfortunately, there are disadvantages of using PVM as a model system to study RSV pathogenesis. For instance, there is no direct cross-reactivity between these two viruses as both pathogens are inherently different (e.g. PVM F protein shares only 40% animo acid sequence identity to that of RSV) [1, 67, 68].

Thus, the study of antigen-specific acquired immunity is very limited [75, 77]. Nevertheless, there are sufficient similarities in the molecular pathogenesis that make PVM suitable for the study of RSV-induced inflammation and severe respiratory disease. Apart from the numerous advantages of using mice in the laboratory, PVM also serves as an appropriate platform for the development of novel approaches to combat severe RSV disease [67, 75].

1.4.2.2 Cattle and Bovine RSV (BRSV)

A natural pathogen of cattle, BRSV is considered a major cause of respiratory disease in calves [1, 67, 68, 74]. The virus was discovered and further described by *Paccaud* and *Jacquier* in 1970 [78]. Since then, it was found that RSV and BRSV are antigenically very similar, with 80% homology between the two viruses [1, 6, 74, 79]. In addition, BRSV-mediated disease in cattle closely resembles that of RSV in humans [6, 67, 80]. For instance, young age is a major factor dictating disease severity in both infection models [1, 67, 81]. BRSV clinical outcomes can range from subclinical to fatal, with worsening of symptoms occurring in calves less than 6 months old [1, 68]. Aerosolized infection of calves with BRSV starts with non-specific symptoms like fever and anorexia, which is then followed by both upper and lower respiratory tract clinical signs like rhinitis, cough, rapid breathing, wheezing, dyspnea, and hypoxemia [1, 67, 68, 74]. Similar to both RSV and PVM, strong neutrophilic infiltration occurs in the lower airways, and recruitment of effector lymphocytes is usually limited [1, 67, 68, 80]. BRSV histopathology in calves is characterized by bronchiolitis, interstitial pneumonia, mucus

overproduction, atelectasis, and in most severe cases, bullous emphysema [1, 67, 68, 81]. High concentrations of TNF-α and IL-6 were detected in the BALF of calves with LRT disease [1, 67, 68, 74]. In contrast to RSV disease in humans, bacterial co-infections with *Mannheimia, Haemophilus* and *Pasteurella* species may occur in cattle infected with BRSV, bovine PIV-3, bovine herpesvirus 1 (BHV-1), and/or bovine viral diarrhea virus (BVDV) [82]. This subsequently leads to what is commonly known as bovine respiratory disease complex (BRDC) [67, 74, 81, 82].

Despite sharing similar genetics, epidemiology and clinical disease features with RSV, the BRSV infection model has several disadvantages. Though the availability of bovine molecular tools and immunological reagents has rapidly increased over the past few decades, it still remains relatively poor compared to that of rodents. In addition, the high cost of calves also limits the use of this model to study RSV pathogenesis [51, 74]. Special veterinary expertise in housing and handling of these animals is required, and more importantly, BRSV and RSV are inherently different pathogens after all [67]. Regardless, the BRSV infection system in a large animal model has all the necessary qualities to successfully assess the efficacy of novel RSV vaccines and therapeutics in preclinical trials [68].

1.5 Immunomodulators

1.5.1 Definition

The appropriate stimulation of the immune system can improve the immediate control of pathogens, especially in situations where this fails at protecting the host from

infection. Immunomodulators are substances known to modify and correct the nature of host's immune responses [83-85]. These agents can be obtained from endogenous or exogenous sources. Examples include cytokines, chemokines, growth factors, immunoglobulins, compounds of synthetic or natural origin, and microbial products [83, 86-88]. Immunomodulators can exert their function in either an antigen-specific or an antigen-independent manner [86, 88]. In addition, they can be further subdivided into immunoadjuvants, immunostimulators, and immunosuppresants [85, 88]. Immunomodulators are currently being used as vaccine adjuvants, as well as in strategies to combat various types of cancers, microbial infections, and autoimmune conditions [83-85, 87, 89].

1.5.2 Applications

Most immunomodulators act at the level of the innate immune system [90]. The engagement of PRRs and their respective signal transduction pathways leads to the induction of the inflammatory response. Vaccine adjuvants are immunomodulators known to enhance the immunogenicity of a particular antigen [91]. These compounds can either be part of the immunogen itself, or be separately added to the formulation [92]. For instance, whole microbial preparations, either attenuated or killed, are thought to have both adjuvant and immunomodulatory properties [88]. The attenuated *Mycobacterium* strain used in the Bacillus Calmette–Guerin (BCG) vaccine is a perfect example of this. It is primarily used for immunization against tuberculosis and leprosy [92]. Additionally, this microbial immunomodulator has also been used in cancer immunotherapies [88, 91].

BCG strain works as an adjuvant because it contains several TLR ligands like peptidoglycans, lipopolysaccharides (LPS), cytosine-phosphate-guanosine oligodeoxynucleotides (CpG ODNs), and flagellin [92]. Furthermore, BCG promotes cell-mediated immune responses against tumor-associated antigens, thus currently being a routine treatment for patients with superficial bladder cancer [91, 93].

Imiquimod, a synthetic imidazoquinoline amine and commercially known as Aldara®, is another example of an immunomodulator used in cancer immunotherapy [94]. Approved by the FDA in 2004, imiquimod is used as a topical ointment for the treatment of primary superficial basal cell carcinoma (BCC) [95]. This compound binds to the endosomal TLR7 of plasmacytoid DCs (pDCs), leading to the production of pro-inflammatory cytokines like IFN-α, TNF- α, IL-12, among others [94, 95]. As a result, skin macrophages and other innate immune cells become activated, releasing reactive oxygen species (ROS) and toxic byproducts [95]. It is thought that high concentrations of imiquimod can lead to the specific apoptosis of tumor cells in the skin [94, 95]. Moreover, the family of imidazoquinolines tends to promote both anti-viral and Th1-biased immune responses *in vivo* [94]. Hence, imiquimod, is also used to treat human papillomavirus (HPV)-induced genital warts [96].

Immunomodulators can also be used to combat microbial infections [84, 86]. The rationale behind this approach originates from the fact that these compounds mediate the activation of immune cells involved in pathogen control and clearance (i.e. macrophages, NK cells, etc) [87]. In addition, immunomodulators can play a role in the regulation of pathogen-induced immunopathology. For instance, a Th1-biased immune response is required for the protection against fungal infections [86, 97]. Immunocompromised

patients lack the ability to mount appropriate immune responses against most pathogens. In the case of human immunodecifiency virus and acquired immune deficiency syndrome (HIV/AIDS) patients, a high proportion of them present with low neutrophil cell counts and other cytopenias in the blood [87, 98]. Thus, these individuals are at a higher risk of acquiring bacterial and fungal infections [87]. According to several clinical studies, colony-stimulating factors (CSFs) are able to revert the state of neutropenia in these individuals [86]. There is evidence that granulocyte-macrophage CSF (GM-CSF) added as an adjunct to amphotericin B therapy decreases mortality rates in neutropenic patients with invasive fungal infections [86, 99]. In addition, macrophage CSF (M-CSF) has been shown to increase antifungal activity of murine macrophages, monocytes and neutrophils [84]. This is important because these effector cells can further complement and synergize with the intrinsic antifungal activity of azole fungistatic drugs [84].

Autoimmunity arises when the mechanisms involved in self-nonself discrimination fail at making such distinction [96]. As a result, exacerbated immune responses are mounted against self-antigens, often leading to severe immunopathologies [100]. Immunomodulators that suppress or neutralize these overzealous responses can ameliorate the symptoms of systemic autoimmune diseases. For instance, the persistent activation of pDCs during systemic lupus erythematosus (SLE) leads to the constant induction of IFN-α [96, 100]. Hence, patients with active SLE tend to have elevated levels of this IFN in the blood [96]. In addition, human pDCs are known to express endosomal TLR7 and TLR9 [100]. It is thought that either self-DNA or immune complexes composed of autoantibodies with RNA binding nucleoproteins can be engulfed by pDCs and serve as ligands for those receptors [96]. Thus, a number of

synthetic ODN antagonists have been generated to specifically inhibit TLR7 and TLR9 signaling transduction pathways [101]. One research group demonstrated that the immunoregulatory sequence (IRS) 954 inhibits both TLR7 and TLR9 signaling in mice [101]. In the context of experimental SLE, animals that received IRS 954 treatment during the onset of SLE had lower autoantibodies in the serum, as well as less symptoms and increased survival than untreated mice [101]. IRS 954 is currently being evaluated in preclinical trials as a potential treatment for SLE in humans [96].

1.5.3 Benefits

Immunomodulators have become an attractive alternative to conventional interventions in many clinical settings. These compounds can provide an optimal innate stimulation of the host's immune system, resulting in a broadened capacity to combat numerous insults. Their benefit stems from their ability to naturally shape innate immune responses via the activation of key PRR signaling pathways. In the context of viral infections, these agents are able to enhance anti-viral immunity by promoting the recruitment of macrophages, DCs, and NK cells, and augmenting the production of IFN proteins [83, 84]. Immunomodulators often cause fewer adverse effects than existing drugs (i.e. antivirals, antibiotics, etc.), are less likely to mediate antimicrobial resistance, and work synergistically with chemotherapeutic compounds. When used as adjuncts in combinational therapies, these can shorten the course of treatment and overall drug dosage. [83-85].

1.6 P-I-P

P-I-P is a novel immunomodulator consisting of polyinosinic-polycytidylic acid (poly I:C), innate defense regulator (IDR) peptide 1002, and poly[di(sodiumcarboxylatoethylphenoxy)]phosphazene (PCEP). Previously, our group demonstrated that when using this immunomodulator as a vaccine adjuvant in combination with a truncated version of the RSV fusion (F) protein, this formulation is able to induce long-lasting mucosal and systemic immune responses against RSV in several animal model systems [102-104]. Based on these data, it is speculated that this immunomodulator has the potential to be employed in applications other than vaccines, as an alternative strategy to prevent or treat infectious diseases.

1.6.1 Poly I:C

Poly I:C is a synthetic analogue of double stranded RNA (dsRNA), considered to be a molecular pattern associated with viral infections [102, 105, 106]. This compound is able to activate the innate immune system via PRR signaling pathways [107]. Notably, poly I:C is mainly recognized by endosomal TLR3 and cytoplasmic RLRs, such as RIG-I and MDA-5 [102, 105-107]. In mammals, TLR3 expression has been detected in multiple cell types like ECs, fibroblasts, tumor cells, keratinocytes, DCs, macrophages and B cells [105, 107]. In contrast, RIG-I and MDA-5 expression is more ubiquitous as almost every tissue expresses it the cytosol [107]. The engagement of poly I:C with these receptors mediates the recruitment and activation of several transcription factors, specifically NF-

κB, IRF3 and IRF7 [105]. Consequently, these signaling events lead to the production of pro-inflammatory cytokines and type I IFNs [102, 105, 107]. In addition, poly I:C can increase the expression of co-stimulatory molecules in antigen-presenting cells (APCs), and promote Th1 immune responses *in vivo* [107-109]. Overall, the intrinsic immunostimulatory properties of poly I:C make it an attractive compound to be use in applications ranging from vaccine adjuvants to cancer immunotherapies.

1.6.2 IDR peptide 1002

IDR peptide 1002 is a synthetic cationic peptide derived from bovine bactenecin, a 12-amino-acid cathelicidin produced by bovine neutrophils [110-112]. Many research groups have described the mechanism of action of such peptides. Both naturally produced and synthetic IDR peptides can interact with G protein-coupled receptors (GPCRs) on the surface of many cells or directly enter into the cytosol through lipid rafts [113]. Once inside the cell, these peptides bind several intracellular receptors like glyceraldehyde 3-phosphate dehydrogenase (GAPDH) and sequestosome-1 (SQSTM1), leading to the activation of multiple signaling pathways involved in the initiation of innate immune responses [113]. Hence, IDR peptides are known to possess a vast array of immunomodulatory activities both *in vitro* and *in vivo,* including induction of cytokine and chemokine production, regulation of host's cellular gene expression, immune activation and apoptosis, modulation and control of the levels of pro-inflammatory cytokines, ROS and toxic byproducts released by immune cells during infection, stimulation of chemotaxis and leukocyte recruitment into the site of infection, promotion

of angiogenesis and wound healing [110, 113, 114]. There is evidence suggesting that IDR peptide 1002 is a better inducer of chemokines *in vitro* than IDR-1, another well-known bactenecin-derived peptide [110, 111, 113]. In addition, IDR peptide 1002 protected mice against invasive *Staphylococcus aureus* and *Escherichia coli* infections by enhancing monocyte and neutrophil recruitment into the site of infection [110, 111, 113]. It is thought that this peptide possesses anti-inflammatory properties, as it is able to suppress pro-inflammatory immune responses *in vivo* [113]. Altogether, the unique biological properties of IDR peptide 1002 confirm its intrinsic immunomodulatory capacity and elucidate its potential at combating human infectious diseases.

1.6.3 PCEP

Polyphosphazenes are high-molecular weight synthetic polymers consisting of an alternating phosphorus-nitrogen backbone with organic side groups attached to each phosphorous atom [115]. The properties of these macromolecules can be easily modified by the incorporation of different ionic moieties to their structural backbone [115, 116]. PCEP is a water-soluble, new generation polyphosphazene polyelectrolyte known to have strong adjuvant activity *in vivo* [116]. According to a number of animal studies, PCEP induces long-lasting immune responses to a variety of bacterial and viral protein antigens [117]. In the context of vaccines, this polyphosphazene has the potential to form non-covalent protein-polymer complexes in solution, promote balanced cell-mediated and humoral immune responses, act as a delivery system, and strongly modulate the early innate immune response at the site of immunization [115, 117-119]. In addition, it has

been shown that intranasal delivery of PCEP with influenza virus X:31 antigen can induce both systemic and mucosal immune responses in mice [117]. One research group revealed that the intramuscular delivery of PCEP in mice activated the NLRP3 inflammasome, along with the production of IL-1β and IL-18 within the tissue [120]. However, the complete mechanism of action of polyphosphazenes *in vivo* remains to be fully elucidated. Nonetheless, these macromolecules are currently being used in several biomedical settings including novel drug delivery systems, adjuvants in vaccine formulations, hydrogel-forming materials for tissue protheses, among others [116].

2. HYPOTHESIS AND OBJECTIVES

Hypothesis:

As mentioned previously, P-I-P has been shown to be a successful adjuvant platform in the context of an RSV vaccine using F protein as protective antigen. Taking into consideration the immunomodulatory properties of this adjuvant platform, we anticipate that the sole stimulation of the innate immune system by the use of this formulation will protect susceptible Balb/c mice against a lethal dose of PVM. Additionally, we predict that the protection induced by P-I-P against PVM disease should pose minimal side effects to the animals.

Objectives:

The first objective is to assess the potential of P-I-P to protect adult Balb/c mice against lethal PVM-15 infection based on clinical disease, survival scores, virus replication and lung histopathology. In addition, we will conduct gene and protein expression studies to quantify key factors involved in host defense in response to P-I-P treatment in the absence of virus challenge.

The second objective is to examine the nature of the inflammatory response induced by P-I-P treatment in order to delineate a possible mechanism of action *in vivo*. We will conduct studies to measure the mRNA and protein expression of cytokines, chemokines, and IFNs in the lungs, as well as the infiltration of neutrophils, alveolar macrophages, DCs, NK cells and eosinophils within the tissue.

Lastly, the third objective is to determine the optimal time of P-I-P treatment to use for prophylaxis. We will monitor clinical scores for weight loss, disease signs and survival.

3. MATERIALS AND METHODS

3.1. Cell line and virus propagation.

PVM-15 was propagated in Baby Hamster Kidney 21 (BHK-21, ATCC, Manassas, VA, USA) cells in Dulbecco's Modified Eagle Medium (DMEM, Sigma-Aldrich, St. Louis, MO, USA) containing 2% fetal bovine serum (FBS, Gibco, Thermo Fisher Scientific, Waltham, MA, USA), 0.1 mM non-essential amino acids (Thermo Fisher Scientific, Waltham, MA, USA), 10 mM HEPES (Thermo Fisher Scientific, Waltham, MA, USA), and 50 μg/ml gentamicin (Thermo Fisher Scientific, Waltham, MA, USA) [13]. These cells were grown to a confluency of ~75-80% in T150 flasks (BD Biosciences, Franklin Lakes, NJ, USA). Then, the medium was removed from the flask and the cell monolayers were gently washed with DMEM. Afterwards, the cells were infected with PVM15 at a multiplicity of infection (MOI) of 0.1 in an initial volume of 5 ml. The infected flasks were immediately placed on top of a rocking platform inside a 37°C room for 1.5 hr. Next, 11 ml of medium were added to each flask and afterwards the cells were incubated at 37°C, 5% CO_2 for 3 days. The virus was harvested by scraping the cell monolayers into the supernatant using a 39 cm Handle/3.0 cm blade cell scraper (Corning Inc., Corning, NY, USA), and pipetting up and down multiple times to further disrupt cellular debris. This mixture was used as viral stock to infect additional flasks of BHK-21 cells or aliquoted, frozen immediately in liquid nitrogen, and stored in an -80°C freezer for long-term use.

3.2. Treatment formulations and challenge of mice with PVM-15.

To determine the effects of P-I-P on the innate responses over time, five to six week-old female Balb/c mice (Charles River Laboratories, Saint-Constant, QC, Canada) were given 20 µl of PBS or P-I-P intranasally, and lungs were collected at selected time points for further analysis. To evaluate the ability of P-I-P to elicit protection from viral infection, five to six week-old female Balb/c mice were given intranasal treatments of PBS or P-I-P, and challenged 1, 3, 4, 5, or 6 days later with PVM. The P-I-P formulation contained phosphate-buffered saline (PBS, Gibco, Thermo Fisher Scientific, Waltham, MA, USA), 20 µg low-molecular weight poly I:C (Invivogen, San Diego, CA, USA), 40 µg IDR peptide 1002 (Genscript, Piscataway, NJ, USA), and 20 µg PCEP (Idaho National Laboratory, Idaho Falls, ID, USA). The 1:2:1 ratio of the P-I-P formulation was previously determined to be optimal when used as an adjuvant [121]. A full description of treatment groups in the experiments is provided in Table 3.1.

On the day of challenge, mice were inoculated intranasally with 3000 pfu of PVM-15 in 50 µl. Animals were placed under light anesthesia with isoflurane during this procedure. Five mice per group were chosen exclusively to be scored and weighed daily according to a pre-established guideline used by our Animal Care unit. A score of 0 is given to mice with weight loss of 0 to 3.9%. A score of 1, 2 and 3 represents a weight loss of 4 to 10.9%, 11 to 19.9%, and greater than 20% respectively. If the latter situation was observed, the animal would be euthanized even if the trial had not yet ended. The remaining mice were used for lung sample collection at various time points throughout the experiment. On the last day of the trial, day 14 post-infection (p.i.), all remaining

mice were euthanized with isoflurane. In some experiments, the lungs of surviving mice were collected on day 14 p.i. for further analysis. All animal trials were conducted according to the guidelines established by the University Committee on Animal Care and Supply (UCAS) at the University of Saskatchewan in accordance with the Canadian Council on Animal Care (CCAC).

Table 3.1: Detailed description of each treatment group in animal trials.

	Treatment Groups	Formulation	Purpose
A	PBS	20 µl PBS as treatment. No challenge.	Gene and protein expression studies in response to P-I-P alone.
B	P-I-P	20 µg LMW poly I:C + 40 µg IDR peptide + 20 µg PCEP in 20 µl as treatment. No challenge.	Gene and protein expression studies in response to P-I-P alone.
C	PBS/Medium	20 µl PBS as treatment. 50 µl medium as challenge.	Protection studies.
D	P-I-P/PVM	20 µg LMW poly I:C + 40 µg IDR peptide + 20 µg PCEP in 20 µl as treatment. 50 µl 3000 pfu PVM as challenge.	Protection studies.
E	PBS/PVM	20 µl PBS as treatment. 50 µl 3000 pfu PVM as challenge.	Protection studies.

3.3. Collection and processing of lung samples.

At 6, 24, 96 and 144 hr post-treatment (p.t.) or on days 0, 3 and 5 p.i., five mice per group per time point were euthanized with an overdose of isoflurane. Lung samples were collected to evaluate virus titers and expression of innate immune response genes and proteins. The single-lobed left lung was clamped off and removed into a 2 ml screwcap tube containing ~1 ml of 2.4 mm zirconia beads (BioSpec Products Inc, Bartlesville, OK, USA) and 1 ml of TRIzol® reagent (Thermo Fisher Scientific, Waltham, MA, USA). This lung was used for mRNA extraction and gene expression studies. The multi-lobed right lung was removed into a tube containing 1 ml of 2.4 mm zirconia beads, and 1 ml of DMEM supplemented with 0.1 mM non-essential amino acids, 10 mM HEPES, 50 μg/ml gentamicin, and 1X antibiotic/antimycotic (Thermo Fisher Scientific, Waltham, MA, USA). These lungs were used for virus titrations, as well as cytokine, chemokine and IFN multiplex ELISAs. Both lungs were homogenized for 10 sec at 4,800 rpm using a mini bead-beater (BioSpec Products Inc., Bartlesville, OK, USA), and centrifuged at 4°C for 1 min at 10,000 x g to remove gross debris. Immediately, all samples were aliquoted, flash-frozen in liquid nitrogen and stored at -80°C.

3.4. Viral titrations and qPCR assays for PVM quantification.

BHK-21 cells were plated on 96-well plates at a confluency of 80%. In separate 96-well dilution plates, 100 μl of the collected lung homogenates were added to the first row of the plates, and seven 10-fold serial dilutions were made in the remaining wells. Then,

100 µl of these dilutions were transferred in duplicates onto the BHK-21 cell monolayers. After 72 hr of incubation at 37°C and 5% CO_2, the cells were fixed with an ice-cold mixture of 3 parts acetone to 1 part methanol. The plates were washed three times with PBS before the blocking step and in between each antibody incubation period. The plates were blocked with 5% goat serum (Thermo Fisher Scientific, Waltham, MA, USA) solution for 30 min, followed by 2.5 hr incubation with a 1:500 dilution of rabbit polyclonal anti-PVM nucleoprotein antibody in 1% goat serum. Finally, a 1:500 dilution of a secondary Alexafluor® 488 goat anti-rabbit antibody (Thermo Fisher Scientific, Waltham, MA, USA) was added to the wells for 1 hr. Viral plaques were visualized and counted using a fluorescent microscope (Carl Zeiss Canada Ltd., Toronto, ON, Canada).

Absolute PVM copy numbers were calculated via quantitative real-time PCR (qPCR) using a 1:5 serial dilution standard curve of stock PVM RNA in nanograms. The primers used were specific to the small hydrophobic (SH) gene of the virus. Unknown RNA concentrations were calculated following the equation of the curve, and copy numbers were determined according to Avogadro's number and the SH gene amplicon size.

3.5. Gene expression analysis of chemokines, cytokines and interferons by qPCR.

Total RNA was extracted from the single-lobed left lung in TRIzol® reagent according to manufacturer's instructions (Thermo Fisher Scientific, Waltham, MA, USA). Complementary DNA (cDNA) synthesis was performed using the QuantiTect Reverse Transcription kit (Qiagen, Venlo, Limburg, Netherlands). qPCR was carried out using FastStart SYBR Green Master (Roche, Basel, Switzerland). The primers (Thermo Fisher

Scientific, Waltham, MA, USA) and annealing temperatures used in the experiments are listed in Table 3.2. The qPCR reactions were performed according to the following parameters: 1st step at 95°C for 10 min, 2nd step repeated 40X initially at 95°C for 15 sec, then annealing temperature for 30 sec, and lastly 72°C for 30 sec. Finally, the 3rd step was repeated 31X starting at 65°C with 1.0°C increments ending at 95°C. This last step was mainly to acquire data for the melt curve analysis. All results were normalized based on the average of the β-actin levels of all PBS or PBS/Medium control animals.

Table 3.2: List of primers used in qPCR experiments.

Target gene	Direction	Sequence	Amplicon size	Annealing Temp (°C)
β-actin	Forward	5' ACTGGGACGACATGGAG 3'	266bp	57.5
	Reverse	5' GTAGATGGGCACAGTGTGGG 3'		
SH	Forward	5' ACCAGCAGCCGTATTGGCACA 3'	102bp	57.5
	Reverse	5' GCTGCAGGCCATTATCAGCGCA 3'		
IFN-γ	Forward	5' TCAAGTGGCATAGATGTGGAAGAA 3'	92bp	57.5
	Reverse	5' TGGCTCTGCAGGATTTTCATG 3'		
IFN-α	Forward	5' CCTGTGTGATGCAACAGGTC 3'	209bp	59.3
	Reverse	5' TCACTCCTCCTTGCTCAATC 3'		
IFN-β	Forward	5' ATCATGAACAACAGGTGGATCCTCC 3'	419bp	63.9
	Reverse	5' TTCAAGTGGAGAGCAGTTGAG 3'		
CXCL10 (IP-10)	Forward	5' ATGACGGGCCAGTGAGAATG 3'	249bp	67.6
	Reverse	5' GAGGCTCTCTGCTGTCCATC 3'		
CCL3 (MIP-1α)	Forward	5' CTTCTCTGTACCATGACACTC 3'	208bp	57.5
	Reverse	5' AGGTCTCTTTGGAGTCAGCG 3'		
CCL2 (MCP-1)	Forward	5' CTTCTGGGCCTGCTGTTCA 3'	127bp	57.5
	Reverse	5' CCAGCCTACTCATTGGGATCA 3'		
CXCL2 (MIP-2)	Forward	5' TGCGCCCAGACAGAAGTCATAGC 3'	129bp	63.9
	Reverse	5' GCTCTAGAGTCAGTTAGCCTTGCCTTTG 3'		
CXCL1 (KC)	Forward	5' ATGAGCTGCGCTGTCAGTGC 3'	247bp	56.3
	Reverse	5' CACCAGACGGTGCCATCAGA 3'		
IL-12β (p40)	Forward	5' GACCCTGCCCATTGAACTGGC 3'	415bp	57.5
	Reverse	5' CAACGTTGCATCCTAGGATCG 3'		
TNF-α	Forward	5' AGGCACTCCCCCAAAAGATG 3'	203bp	57.5
	Reverse	5' CTGCCACAAGCAGGAATGAG 3'		
IL-1β	Forward	5' GTGTGGATCCCAAGCAATAC 3'	173bp	55.0
	Reverse	5' GTCCTGACCACTGTTGTTTC 3'		

IL-6	Forward	5’ GTGGCTAAGGACCAAGACCA 3’	95bp	59.2
	Reverse	5’ TAACGCACTAGGTTTGCCGA 3’		
IL-10	Forward	5’ GCTGCCTGCTCTTACTGACT 3’	81bp	57.5
	Reverse	5’ CTGGGAAGTGGGTGCAGTTA 3’		
TGF-β	Forward	5’ AGGGCTACCATGCCAACTTC 3’	168bp	57.5
	Reverse	5’ CCACGTAGTAGACGATGGGC 3’		

3.6. Multiplex ELISAs for quantification of chemokine, cytokine and interferon proteins in the lung.

The multi-lobed right lungs of 5 mice per group per time point were individually collected, homogenized in DMEM, aliquoted with 1X SIGMA*FAST*™ Protease Inhibitor solution (Sigma-Aldrich, St. Louis, MO, USA) and flash-frozen on days 0, 3 and 5 p.i. The MSD Multi-Spot V-PLEX assay for the pro-inflammatory panel 1 (TNF-α, IL-1β, IL-6, IL-12, IL-10 and CXCL1) and the MSD Multi-Array Mouse Cytokine Ultra-sensitive Assay for CCL2 were used to quantify cytokine, type II IFN, and chemokine levels in the lungs according to manufacturer's instructions (Meso Scale Discovery, Rockville, MD, USA).

3.7. Cell influx analysis by flow cytometry.

Both multi- and single-lobed lungs were perfused with 5 ml of Hanks balanced salt solution (HBSS, Thermo Fisher Scientific, Waltham, MA, USA) containing 5% FBS. Then, the tissues were mechanically disrupted using a gentle MACS dissociator according to the manufacturer's instructions (Miltenyi Biotec Inc., San Diego, CA, USA). Next, the homogenate was incubated with 0.5 mg/ml of collagenase type IA and 20 μg/ml of type IV bovine pancreatic DNase (Sigma-Aldrich, St. Louis, MO, USA) for 20 min at 37 °C in HBSS containing 5% FBS. After digestion, contaminating red blood cells were lysed by adding room temperature ACK lysing buffer (Thermo Fisher Scientific, Waltham, MA, USA) for 2 min. Cells were washed with PBS + 0.5% bovine serum

albumin (BSA, Thermo Fisher Scientific, Waltham, MA, USA) and subsequently passed through a 40 µm nylon cell strainer (Thermo Fisher Scientific, Waltham, MA, USA). Total cell numbers were determined using a Beckman Coulter Counter (Beckman Coulter Inc., Pasadena, CA, USA). To identify the different leukocyte populations in the lung, cells were first blocked with 2 µl TrueStain fcX (Biolegend, San Diego, CA, USA) for 5-10 min on ice in a 96U-bottomed plate. Subsequently, cells were stained and incubated with their corresponding fluorochrome-conjugated antibody cocktails (Table 3.3) for 20 min on ice in the dark. After three washing steps, cells were fixed with 2% formaldehyde (Sigma-Aldrich, St. Louis, MO, USA) and stored at 4 °C protected from light. Flow cytometry was performed using a FACS Calibur (BD Biosciences, Franklin Lakes, NJ, USA). Analysis of flow cytometry data was performed using Kaluza software (Beckman Coulter Inc., Pasadena, CA, USA).

Table 3.3: List of antibodies used for flow cytometry experiments.

Cell type	Cell surface marker	Isotype	Clone	Supplier
Alveolar Macrophages	FITC anti-mouse CD11c.	Armenian Hamster IgG	N418	Biolegend
	PE anti-mouse Siglec-F.	Rat IgG2a, k	E50-2440	BD Biosciences
	APC anti-mouse I-A/I-E (MHC II).	Rat IgG2b, k	M5/114.15.2	Biolegend
DCs	FITC anti-mouse CD11c.	Armenian Hamster IgG	N418	Biolegend
	APC anti-mouse I-A/I-E (MHC II).	Rat IgG2b, k	M5/114.15.2	
Neutrophils	FITC anti-mouse/human CD11b.	Rat IgG2b, k	M1/70	Biolegend
	APC anti-mouse Ly-6G/Ly-6C (Gr-1).	Rat IgG2b, k	RB6-8C5.	
Eosinophils	FITC anti-mouse CD11c.	Armenian Hamster IgG	N418	Biolegend
	PE anti-mouse Siglec-F.	Rat IgG2a, k	E50-2440	BD Biosciences
	APC anti-mouse CD45.	Rat IgG2b, k	30-F11	Biolegend
NK cells	FITC anti-mouse CD3.	Rat IgG2b, k	17A2	Biolegend
	APC anti-mouse CD335 (NKp46).	Rat IgG2a, k	29A1.4	

3.8. Lung histology.

The multi-lobed right lung was perfused with 10% neutral buffered formalin (NBF, VWR, Radnor, PA, USA) and collected on day 6 p.i. The dissected tissues were submerged in NBF and were allowed to shake for 2 days. Then, the lungs were transferred into cassettes and subsequently immersed in NBF. The perfused lungs were embedded in paraffin, sectioned into duplicate 5 μm sections, stained with hematoxylin and eosin (H & E), and scored in a blinded manner by a veterinary pathologist. Scores were given based on the presence, severity, and distribution of lesions in each lung lobe. Histopathological lesions were characterized by cellular infiltration and edema around blood vessels, bronchi and alveoli. A score of 0 denotes a normal lung, 1 indicates signs of mild perivascular edema, perivasculitis, and limited cellular infiltration within the pulmonary parenchyma, while a score of 2 denotes moderate perivascular edema, perivasculitis, and limited cellular infiltration within the pulmonary parenchyma. Finally, a score of 3 represents severe perivascular edema, perivasculitis, and limited cellular infiltration within the pulmonary parenchyma.

3.9. Statistical analysis.

GraphPad Prism 6 was used to analyze all the data (GraphPad Software, Inc., La Jolla, CA, USA). Differences among the groups as well as between time points were assessed using Student t-tests and the Newman-Keuls method for multiple comparisons. One-way ANOVAs were used to determine differences between the P-I-P/PVM and

PBS/PVM groups in flow cytometry experiments. Differences were considered significant at $P<0.05$.

4. RESULTS

4.1. P-I-P mediates gene and protein expression of chemokines and cytokines involved in host's innate immune responses.

Mice were treated intranasally with P-I-P in order to monitor gene and protein expression profiles of cytokines and chemokines at 6, 24, 96 and 144 hr p.t. Highest mRNA expression was detected at 24 hr p.t. for CCL2, CCL3, CXCL2, and CXCL1 (Fig. 4.1). For the IFN-γ-inducible protein 10, or CXCL10, the highest mRNA expression was observed as early as 6 hr p.t. It is important to note that there was a statistically significant decrease in chemokine mRNA levels between the 24- and 96-hr time points ($p=0.0079$ for CCL2, CXCL2, CXCL1 and CXCL10 and $p=0.0317$ for CCL3), although at the latest time-point assayed (i.e. 144 hr p.t.), chemokine mRNA levels were still upregulated compared to the PBS group. This change was expected, as these molecules tend to have short half-lives *in vivo.*

In terms of pro-inflammatory cytokine gene expression profiles, P-I-P treatment induced moderate upregulation of TNF-α, IL-1β, IL-6 and IL-12β mRNA at 6 and 24 hr p.t. Subsequently, these levels decreased and remained constant with a median normalized fold-change under ~15-fold for most cytokines. TGF-β mRNA levels remained constant and were comparable to those in the PBS group. Interestingly, IL-10 mRNA expression started with a moderate upregulation of less than 10-fold at 6, 24, and 96 hr p.t., and then these levels further increased to approximately 34-fold at the 144 hr

time point. The unique profile of IL-10 mRNA can be attributed to its role in dampening immune responses *in vivo*.

With regards to IFN-α/β and IFN-γ genes, highest mRNA expression was detected from 6 to 24 hr p.t., similar to the trends observed for the chemokine and cytokine genes. The highest level of IFN-α mRNA expression was at 24 hr p.t. Maximal IFN-β mRNA expression occurred earlier than that of IFN-α, at 6 hr p.t. ECs are the main constituent of the lung anatomy and are also a major source of IFN-β in the tissue. Thus, the fact that IFN-β mRNA levels were upregulated as early as 6 hr is not surprising. ECs are often considered the first line of defense of the lung and must respond to insults as early as it is physiologically possible. Additionally, ECs do not need to migrate from other body sites to exert their activity, which is in agreement with the earlier mRNA expression of this IFN. IFN-γ mRNA reached its peak at 6 hr p.t., with a median normalized fold-change of 58.65. By 24 hr p.t., the mRNA levels of this IFN strongly declined. Overall, these data suggest that P-I-P is a good inducer of the IFN response, and could generate an anti-viral state capable of protecting the animals from a lethal infection.

	PBS				P-I-P			
	6 hr p.t.	**24 hr p.t.**	**96 hr p.t.**	**144 hr p.t.**	**6 hr p.t.**	**24 hr p.t.**	**96 hr p.t.**	**144 hr p.t.**
CCL2	0.97	1.16	0.93	0.99	67.65	94.88	19.92	24.59
CCL3	1.86	0.91	1.13	1.29	7.7	15.22	6.18	4.02
CXCL2	2.3	1.14	0.96	1.06	10.7	14.56	2.12	4.14
CXCL1	0.93	1.17	0.9	1.04	23.39	32.67	4.2	6.31
CXCL10	2.12	1.02	1.23	1.18	1765.67	329.01	29.12	19.11
TNF-α	1.59	1.14	0.97	0.99	11.88	7.7	3.83	6.69
IL-1β	0.56	0.97	1.02	1.3	16.73	13.18	1.84	2.03
IL-6	0.88	0.97	1.37	0.99	50.49	44.02	7.02	7.34
IL-12β (p40)	2.02	1.04	1.06	0.88	14.58	13.91	14.34	7.7
IL-10	1.60	1.23	1.04	1.18	9.22	7.78	4.28	33.78
TGF-β	1.14	0.86	1.29	1.22	0.97	1.77	0.76	0.58
IFN-α	1.07	1.32	0.94	1.28	9.62	51.13	1.55	0.69
IFN-β	1.02	1.23	1.07	0.85	278.59	195.09	11.2	4.46
IFN-γ	1.08	1.07	1.11	0.99	58.65	6.32	2.73	9.32

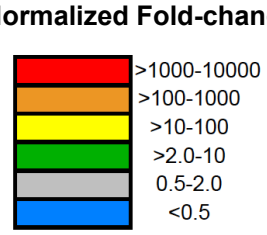

Figure 4.1: Heat map of chemokine and cytokine mRNA expression profiles in the single-lobed lungs of 5-6 week-old female Balb/c mice at 6, 24, 96 and 144 hr p.t. with either P-I-P or PBS. Each treatment group contained 20 mice in total, with sampling of 5 animals at each time-point indicated above. All Ct values were normalized against the average of the β-actin levels of control animals for each specific time point indicated above. Normalized fold-change calculations were performed using the $2^{-\Delta\Delta Ct}$ method. Data are shown as the median of five biological replicates.

In order to confirm and complement the results obtained from qPCR analysis, the total amount of chemokine, cytokine and IFN proteins in lung homogenate supernatants of mice treated with P-I-P was quantified. It is important to note that due to the nature of our samples, availability and sensitivity of the electrochemiluminescence multiplex ELISA kits, we were able to only measure selected chemokines, cytokines, and IFNs at the protein level. Similar to the mRNA expression data (Figs. 4.2A, 4.2C), CCL2 and CXCL1 proteins were highly expressed within the first 24 hr following P-I-P treatment, with concentrations between 3000-5000 pg/ml. At the 96-hr time point, the levels of these chemokine proteins decreased by approximately 86 to 88% with p= 0.0079 (400-600 pg/ml) and during the last time point assayed, the protein concentration of CCL2 increased to 920 pg/ml with p=0.0317 (Figs. 4.2B, 4.2D).

The pro-inflammatory cytokine proteins TNF-α, IL-1β, and IL-6 had a slightly different trend than their mRNA (Figs. 4.2E, 4.2G, 4.2I). Highest protein concentrations were detected at 6 hr p.t., and at 24 hr p.t. These amounts decreased by 90%, 57% and 82%, respectively, when compared to their previous values (p=0.0079). At 96 hr p.t., the levels of these cytokines continued to further decrease (p=0.0079). Notably, the decrease in protein concentration was most pronounced for IL-6, which went from 692 pg/ml to 28.4 pg/ml within 72 hr. Similar to the chemokines, TNF-α, IL-1β, and IL-6 protein concentrations increased approximately 3-fold with p=0.0317 for TNF-α and p=0.0079 for IL-1β, and IL-6 at the 144-hr time point (Figs. 4.2F, 4.2H, 4.2J).

The IL-12 p70 protein concentration was 75 pg/ml at 6 hr after P-I-P treatment. During the next two time points (i.e. 24 and 96 hr p.t.), its quantity was significantly reduced by 38% and 90%, respectively (p=0.0079). At 144 hr, IL-12 p70 protein levels

remained constant (Fig. 4.2L). This trend is different from that of the mRNA (Fig. 4.2K) as in the latter we measured a subunit of the final heterodimer of IL-12 (i.e. p40 subunit), whereas in the former we measured total IL-12 as a heterodimer, or the combination of both p35 and p40 subunits (i.e. p70). The IL-10 protein concentrations were less than 5 pg/ml during the first three time points following treatment, but at 144 hr p.t., there was a significant increase in protein expression, with a median concentration of 30.8 pg/ml ($p=0.0079$) (Fig. 4.2N). This pattern coincides with that observed at the mRNA level (Fig. 4.2M). Indeed, IL-10 is expressed at a later time point presumably because it dampens immune responses to prevent uncontrolled inflammation.

IFN-γ showed a similar trend to that of the pro-inflammatory cytokines, with a starting concentration of 19.54 pg/ml, followed by a decrease of 85% ($p=0.0079$) at 24 hr p.t. During the last time point assayed, there was a 35-fold increase in IFN-γ protein level relative to the 96 hr time point ($p=0.0079$), resulting in a final concentration of 24.6 pg/ml (Fig. 4.2P). This last event was similar to IL-10 protein expression, which was highest at 144 hr p.t.

Collectively, we can conclude that the effect of P-I-P treatment is evident both at the mRNA and protein levels, with similar trends observed for both types of biomolecules. P-I-P-induced inflammation was short-lived, as both mRNA levels and protein concentrations were high within the first 24 hr following treatment, and then declined. While protein levels for chemokines and pro-inflammatory cytokines were slightly elevated at 144 hr p.t. compared to levels detected at the 96-hr time point, highest expression was detected between 6 to 24 hr p.t. It is likely that this minimal increase in protein concentration is not biologically significant. Only for IL-10 and IFN-γ, the

highest expression was measured at the latest time point (i.e. 144 hr p.t.), which suggests a different source of cells recruited by the P-I-P treatment.

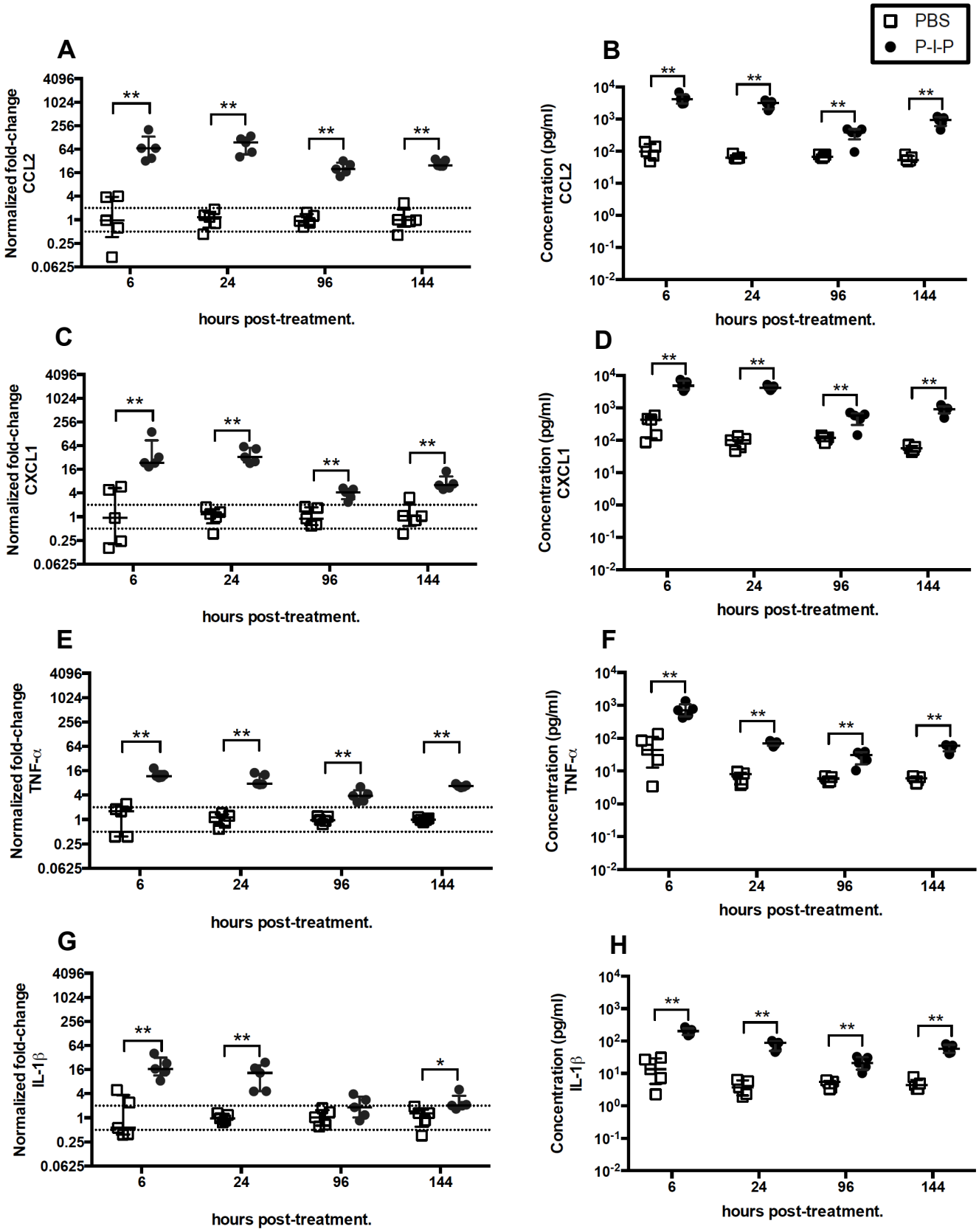
A
Normalized fold-change CCL2
4096
1024
256
64
16
4
1
0.25
0.0625
6
24
96
144
hours post-treatment.
**
B
PBS
P-I-P
Concentration (pg/ml) CCL2
10^4
10^3
10^2
10^1
10^0
10^{-1}
10^{-2}
C
Normalized fold-change CXCL1
D
Concentration (pg/ml) CXCL1
E
Normalized fold-change TNF-α
F
Concentration (pg/ml) TNF-α
G
Normalized fold-change IL-1β
*
H
Concentration (pg/ml) IL-1β

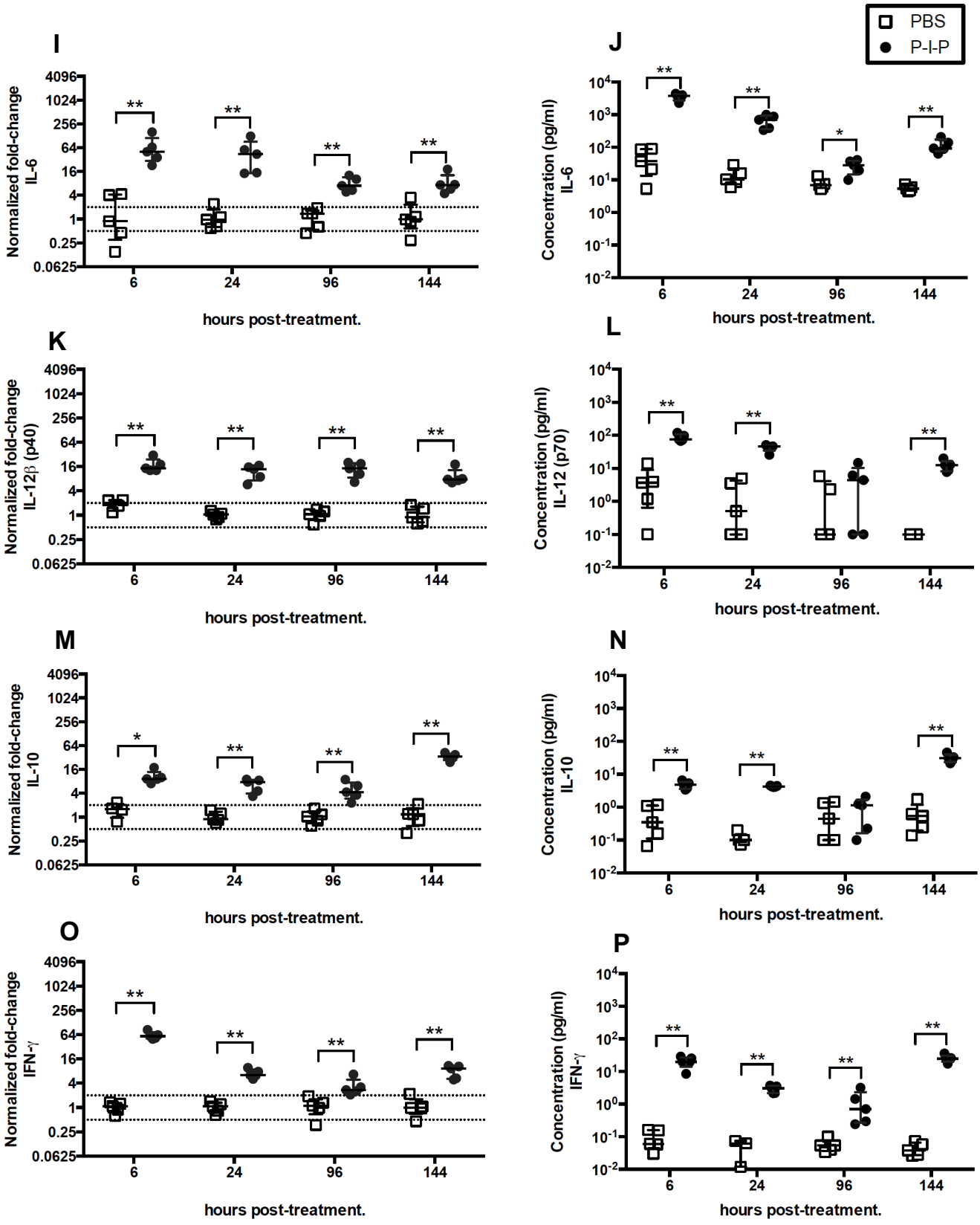
I
J
K
L
M
N
O
P
PBS
P-I-P
Normalized fold-change IL-6
Concentration (pg/ml) IL-6
Normalized fold-change IL-12β (p40)
Concentration (pg/ml) IL-12 (p70)
Normalized fold-change IL-10
Concentration (pg/ml) IL-10
Normalized fold-change IFN-γ
Concentration (pg/ml) IFN-γ
4096
1024
256
64
16
4
1
0.25
0.0625
10^4
10^3
10^2
10^1
10^0
10^{-1}
10^{-2}
6
24
96
144
hours post-treatment.
**
*

Figure 4.2: Comparison between lung mRNA and protein expression levels of chemokine and cytokine genes at 6, 24, 96 and 144 hr p.t. Mice were given intranasal treatment of PBS or P-I-P and the single- and multi-lobed lungs of 5 mice per group per time point were collected separately for each individual animal at the time points indicated. Gene expression was assayed by qPCR, and protein expression by electrochemiluminescence-based multiplex ELISAs. Panels A, C, E, G, I, K, M, and O show mRNA expression for CCL2, CXCL1, TNF-α, IL-1β, IL-6, IL-12β (p40), IL-10, and IFN-γ, respectively. All Ct values were normalized against the average of the β-actin levels of control animals for each specific time point indicated above. Normalized fold-change calculations were performed using the $2^{-\Delta\Delta Ct}$ method. Two horizontal dotted lines at 0.5- and 2-fold were generated to indicate downregulation and upregulation, respectively. Panels B, D, F, H, J, L, N and P represent protein expression data in pg/mL for CCL2, CXCL1, TNF-α, IL-1β, IL-6, total IL-12 (p70), IL-10, and IFN-γ, respectively. Data are shown as individual values representing single animals as well as median with interquartile range of five biological replicates. Only statistically significant differences were indicated in the plots. * $p<0.05$ and ** $p<0.01$.

4.2. P-I-P protects adult Balb/c mice against a lethal PVM infection.

Subsequently, we examined the efficacy of P-I-P pre-treatment at protecting Balb/c mice from lethal PVM challenge. We chose to deliver the treatment 24 hr prior to virus inoculation as during this time point, chemokine and cytokine mRNA and protein levels were high yet displaying a more balanced profile than that detected at 6 hr p.t. Figure 4.3 illustrates the effects of P-I-P pre-treatment on weight loss, mortality, and clinical scores of mice lethally infected with PVM. Of note, animals treated with P-I-P 24 hr prior to virus challenge exhibited minimal weight loss, no overt signs of clinical disease, and 100% survival by day 14 p.i. In regards to virus titers, P-I-P-treated animals had significantly lower numbers of viable virions as well as viral mRNA copies in their lungs when compared to the PBS-treated group (Figs. 4.4A, 4.4B). On day 14 p.i., lung homogenate supernatants of survivor mice were PCR-negative for PVM mRNA copy numbers, suggesting that P-I-P pre-treatment promotes the complete clearance of the virus *in vivo*.

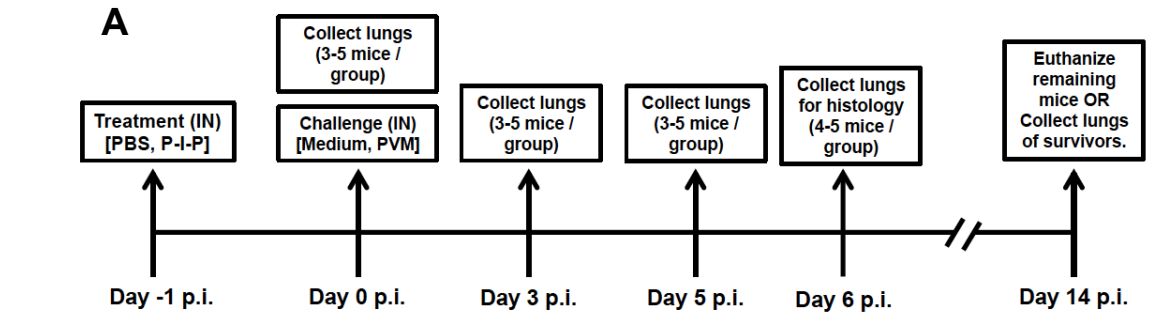
A
Collect lungs (3-5 mice / group)
Treatment (IN) [PBS, P-I-P]
Challenge (IN) [Medium, PVM]
Collect lungs (3-5 mice / group)
Collect lungs (3-5 mice / group)
Collect lungs for histology (4-5 mice / group)
Euthanize remaining mice OR Collect lungs of survivors.
Day -1 p.i.
Day 0 p.i.
Day 3 p.i.
Day 5 p.i.
Day 6 p.i.
Day 14 p.i.

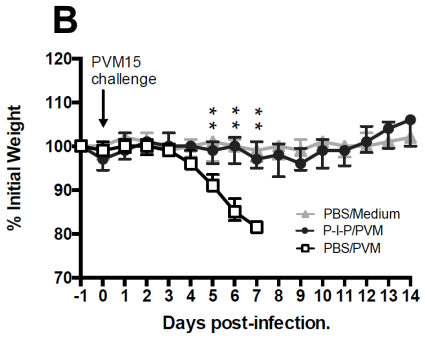
B
PVM15 challenge
% Initial Weight
PBS/Medium
P-I-P/PVM
PBS/PVM
Days post-infection.

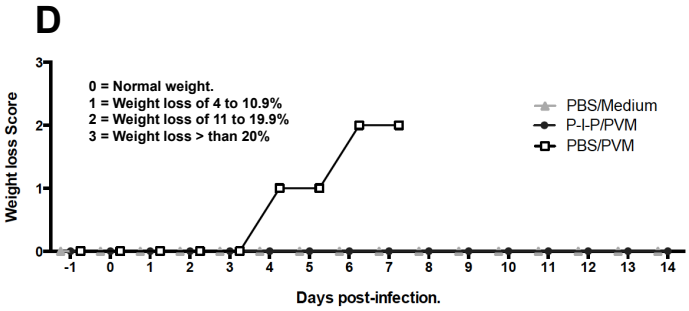
D
0 = Normal weight.
1 = Weight loss of 4 to 10.9%
2 = Weight loss of 11 to 19.9%
3 = Weight loss > than 20%
Weight loss Score
PBS/Medium
P-I-P/PVM
PBS/PVM
Days post-infection.

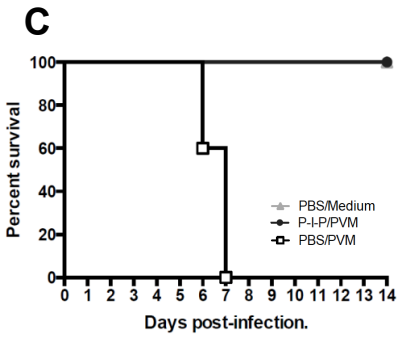
C
Percent survival
PBS/Medium
P-I-P/PVM
PBS/PVM
Days post-infection.

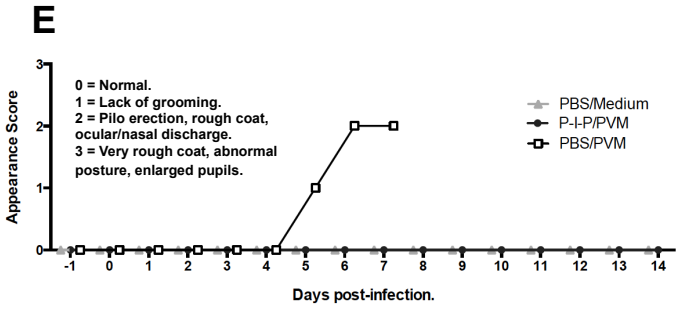
E
0 = Normal.
1 = Lack of grooming.
2 = Pilo erection, rough coat, ocular/nasal discharge.
3 = Very rough coat, abnormal posture, enlarged pupils.
Appearance Score
PBS/Medium
P-I-P/PVM
PBS/PVM
Days post-infection.

Figure 4.3: Outline of trial, weight change, clinical and survival scores of P-I-P- or PBS-treated Balb/c mice before and after intranasal PVM challenge. Mice were given intranasal treatment of PBS or P-I-P 24 hr prior to challenge with 3000 pfu PVM. Animals were weighed and scored before treatment (i.e. day -1), on the day of challenge (i.e. day 0), and for 14 days after infection. Panel A highlights the events occurring in the animal trial. Collection of lung tissue for virus titrations, cell influx and mRNA/protein expression studies was scheduled on days 0, 3 and 5 p.i. Lung samples for histopathology studies were collected on day 6 p.i. On day 14 p.i., qPCR was performed on survivor mice to determine their PVM status. Panel B illustrates weight loss of mice following P-I-P treatment and PVM infection as a median percentage of the starting weight with error bars indicating the interquartile range. The stars indicate statistically significant differences between P-I-P/PVM and PBS/PVM groups. Panel C represents survival rates as the median percentage of the total number of animals per group during the 14 days following infection. Panels D and E show clinical scores for weight loss and appearance represented by the median value for each group throughout the entire animal trial. Each experiment was performed twice and all graphs illustrate the combined results of these two sets of experiments. The total number of animals equals to 10 per group, with an n = 5 for each experiment. ** $p<0.01$.

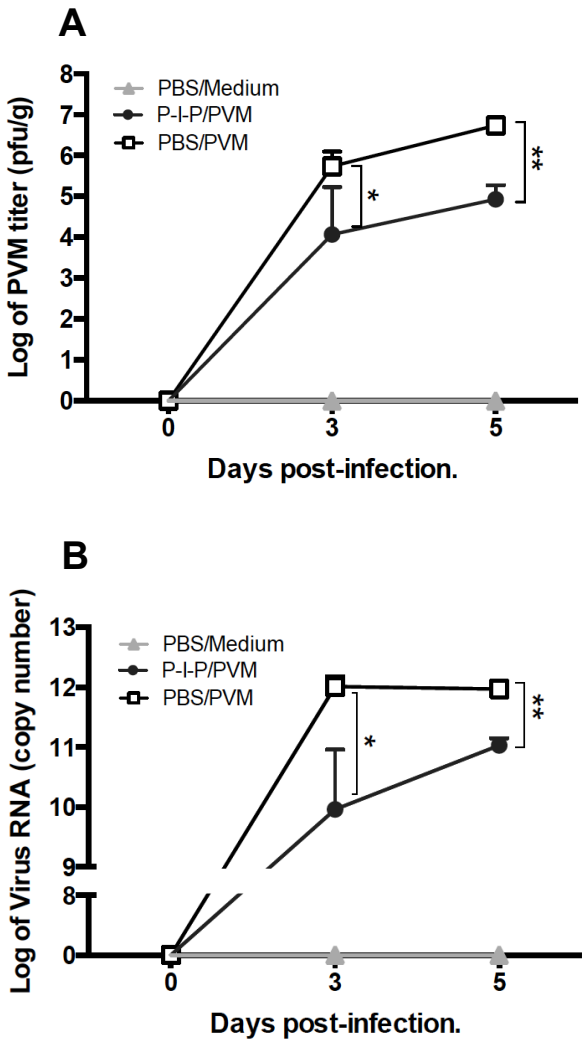

Figure 4.4: PVM titers and absolute virus copy numbers in the lungs of P-I-P pre-treated Balb/c mice on days 0, 3 and 5 p.i. The multi-lobed lung was homogenized in DMEM and used for virus titrations. Panel A shows the log of PVM titers in the lung tissue expressed in pfu/g. The single-lobed lung was processed in TRIzol and used for qPCR. Panel B shows the log of absolute PVM mRNA copy numbers, which were determined as described in the Materials and Methods section. Data are represented as the median with interquartile range of five biological replicates per group. Each experiment was performed twice. * $p<0.05$, ** $p<0.01$.

4.3. P-I-P reduces lung lesions as well as influx of neutrophils and eosinophils into the lungs of Balb/c mice lethally infected with PVM.

The lung pathology induced by PVM infection in P-I-P- and PBS-treated mice was examined in a subsequent trial. Treatment and challenge was delivered as previously described (Table 3.1) and lung sample collection was performed on day 6 p.i. A veterinary pathologist scored the lung sections in a blinded fashion based on severity of lesions, with 0 being normal and 3 being the worst outcome. The lung architecture of the control group (i.e. PBS/Medium) was normal with clear airways and alveoli, suggesting no signs of disease (Figs. 4.5A, 4.5B). The lungs of the P-I-P/PVM group showed signs of multifocal peribronchiolitis, perivasculitis and greater infiltration of leukocytes into the airways than the PBS/Medium control animals (Figs. 4.5C, 4.5D). Nonetheless, there were no signs of edema and hemorrhage in these mice. As shown in figures 4.5E to 4.5G, the PBS/PVM group had areas of acute to subacute alveolitis, multifocal to locally extensive, and severe perivasculitis with edema and hemorrhage in their lungs. Panels 4.5F and 4.5G illustrate an enclosed region of edema of the lung. It can be noted that a large proportion of the infiltrating cells are polymorphonuclear leukocytes (PMNs) mostly in the form of neutrophil granulocytes. Edema was observed in all PBS-treated PVM-infected mice, whereas hemorrhage was only detected in 2 out of 5 mice. There was a statistically significant difference in lung pathology scores between P-I-P-treated and PBS-treated PVM-infected mice, suggesting that treatment with P-I-P reduces the amount and severity of lesions in the lungs following an otherwise lethal PVM infection (Fig. 4.5H).

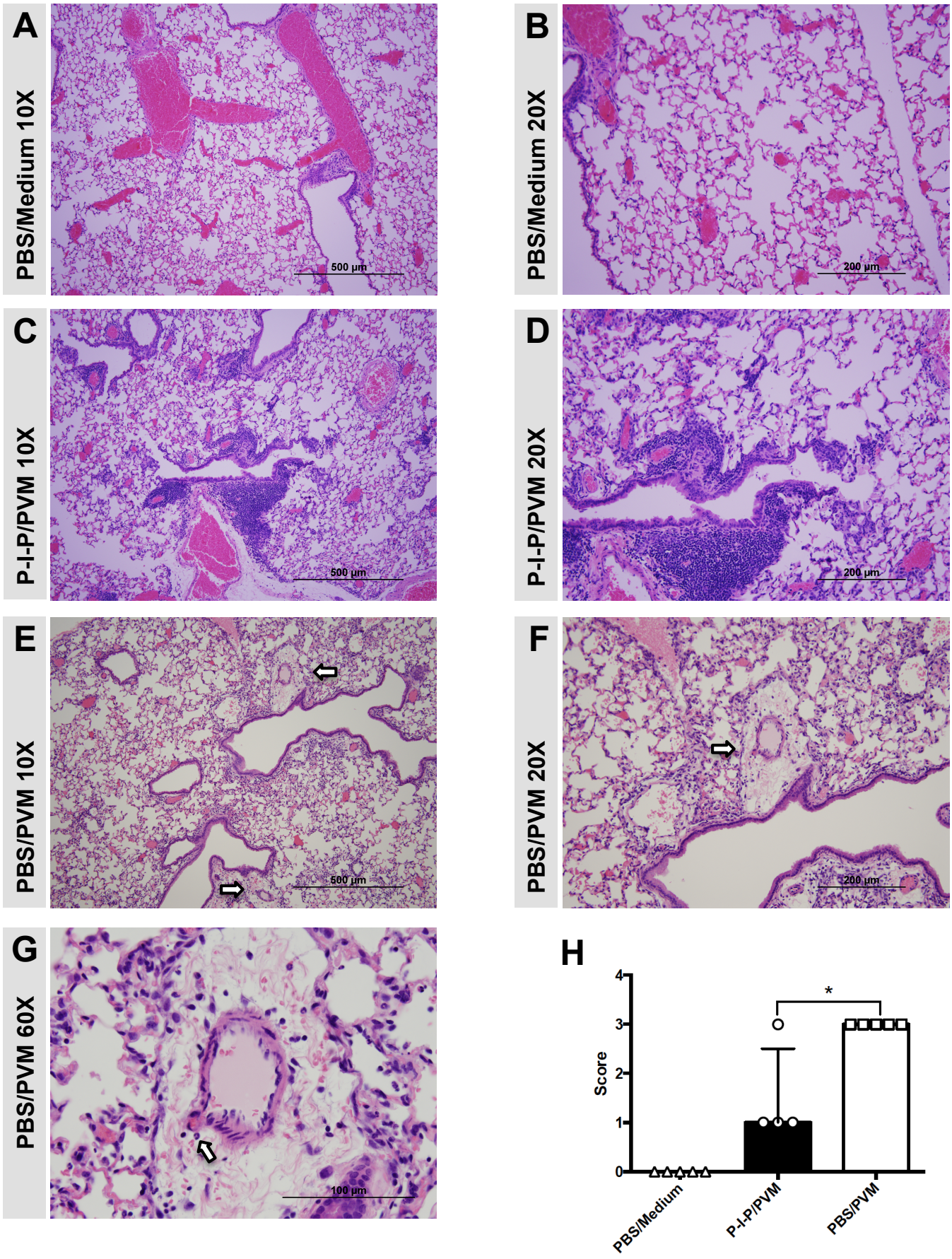
A
PBS/Medium 10X
500 µm
B
PBS/Medium 20X
200 µm
C
P-I-P/PVM 10X
500 µm
D
P-I-P/PVM 20X
200 µm
E
PBS/PVM 10X
500 µm
F
PBS/PVM 20X
200 µm
G
PBS/PVM 60X
100 µm
H
Score
0
1
2
3
4
*
PBS/Medium
P-I-P/PVM
PBS/PVM

Figure 4.5: Lung pathology of Balb/c mice pre-treated with P-I-P or PBS 24 hr prior to lethal intranasal PVM challenge. Four to five mice per group were treated as described in figure 3 and infected intranasally with 3000 pfu of PVM. All lung samples were collected on day 6 p.i. Panels A & B represent lung sections at 10X and 20X magnifications, respectively, for the PBS/Medium control group. Panels C & D show lung sections at 10X and 20X magnifications, respectively of mice treated with P-I-P. Panels E to G illustrate lung sections of PBS-treated PVM-infected mice at 10X, 20X or 60X magnification, respectively. White arrows point to several areas of edema in the tissue, as well as PMNs within this region. Panel H shows the lung histopathology scores given on the basis of the severity and dissemination of the lesions visible in duplicate lung sections. Data are represented as both individual and median values for each group with error bars indicating the interquartile range. * $p<0.05$.

In view of the significant infiltration of PMNs into the lungs of PBS-treated PVM-infected mice, this phenomenon was further explored by measuring the influx of different innate immune cells into the lungs based on specific cell surface markers. The cells assayed were alveolar macrophages ($CD11c^{+}$, $MHCII^{low}$, $SiglecF^{+}$), DCs ($CD11c^{+}$, $MHCII^{high}$), neutrophils ($CD11b^{+}$, $Gr\text{-}1^{+}$), NK cells ($CD3^{-}$, $NKp46^{+}$) and eosinophils ($CD45^{+}$, $CD11c^{-}$, $SiglecF^{+}$). P-I-P-treated mice showed increased numbers of alveolar macrophages on day 0 p.i., which peaked on day 3 p.i. By day 5 p.i., these values had leveled off and were comparable to those of both control and PBS-treated PVM-infected mice (Fig. 4.6A). In terms of DCs, P-I-P treatment significantly increased the early migration of these cells into the lungs as compared to the PBS-treated PVM-infected animals. DC influx in P-I-P-treated mice increased over time and was significantly higher than the numbers detected in PBS-treated PVM-infected mice (Fig. 4.6B).

Additionally, neutrophil infiltration in P-I-P-treated animals was characterized by an early transient recruitment into the lungs after PVM infection, and during later time points, these numbers tended to decrease and level off thereafter. In contrast, PBS-treated PVM-infected mice started with low neutrophil counts, and as the infection progressed, these values significantly increased over time (Fig. 4.6C). On day 5 p.i., PBS-treated PVM-infected mice had greatly elevated levels of neutrophils in the lungs, suggesting a possible neutrophilia, which was also confirmed and noted based on the histology shown in figures 4.5E to 4.5G. Eosinophil influx patterns of PBS-treated PVM-infected mice were similar to those of the neutrophils during days 3 and 5 after PVM challenge. Eosinophil numbers went up on day 3 p.i., and continued to significantly increase thereafter. However, P-I-P-treated animals display a pattern of eosinophil recruitment

similar to that of the PBS/Medium group. Thus, it is evident that PBS-treated PVM-infected mice showed signs of eosinophilia, whereas P-I-P-treated animals did not (Fig. 4.6D). Lastly, P-I-P treatment induced early recruitment of NK cells into the lungs on day 0 p.i. By days 3 and 5 p.i., cell influx decreased, reaching numbers comparable to those in the PBS/Medium group. Interestingly, PBS-treated PVM-infected mice showed an opposite trend. These animals had delayed NK cell recruitment, with highest numbers on day 5 p.i. It is worth mentioning that at this time point, NK cell numbers were significantly higher in the PBS-treated PVM-infected mice compared to the P-I-P-treated group (Fig. 4.6E).

Overall, P-I-P treatment induced early influx of cells that play key roles in the induction and regulation of antiviral innate immunity, such as NK cells, DCs, and alveolar macrophages. Additionally, P-I-P treatment reduced the excessive recruitment of cells associated with immunopathology, namely neutrophils and eosinophils, after PVM infection.

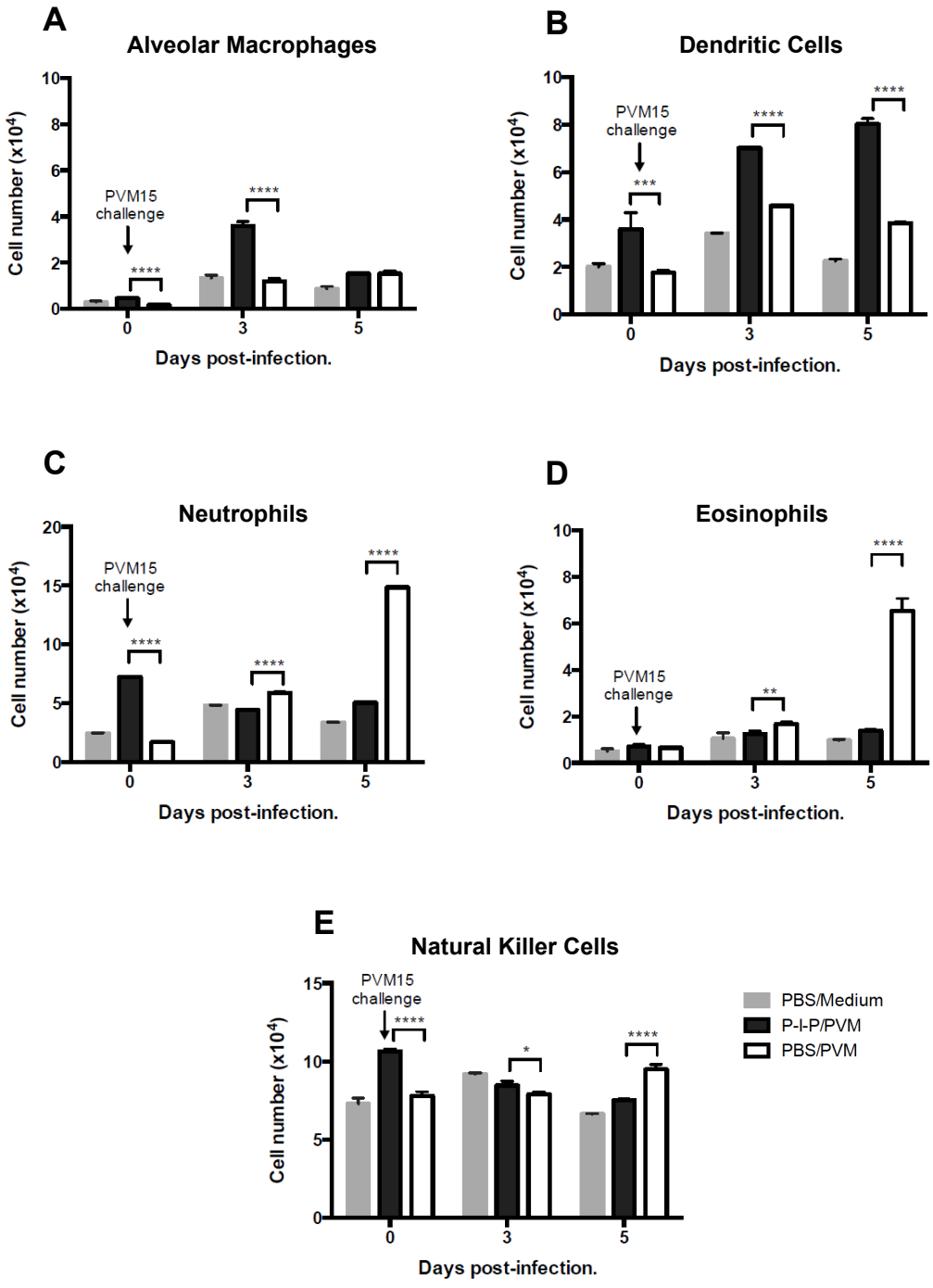
A
Alveolar Macrophages
Cell number (x10⁴)
PVM15 challenge
****
Days post-infection.
B
Dendritic Cells
PVM15 challenge
***
****
C
Neutrophils
D
Eosinophils
**
E
Natural Killer Cells
*
PBS/Medium
P-I-P/PVM
PBS/PVM

Figure 4.6: Infiltration of various immune cells into the lungs of P-I-P pre-treated Balb/c mice on days 0, 3 and 5 following lethal PVM challenge. Mice were given an intranasal treatment of PBS or P-I-P 24 hr prior to challenge with 3000 pfu PVM. The lungs of 3 mice per group were collected, pooled, and processed at the time points indicated. Following physical and chemical digestion of the tissue, single-cell suspensions were acquired. Total numbers of alveolar macrophages (A), DCs (B), neutrophils (C), eosinophils (D), and NK cells (E) in the lungs were analyzed by flow cytometry. Results are presented as cell number x 10^4 per million cells. Data are shown as the median with interquartile range of three technical replicates per cell type assayed. Only statistically significant differences between P-I-P/PVM and PBS/PVM groups are indicated in the plots. * $p<0.05$, ** $p<0.01$, *** $p<0.001$ and **** $p<0.0001$.

4.4. P-I-P pre-treatment promotes early upregulation of chemokines, pro-inflammatory cytokines and interferons, shifting the overall nature of immune responses against PVM.

We examined the nature of the immune responses induced by P-I-P in terms of mRNA and protein expression levels of selected chemokines, cytokines and IFN molecules involved in PVM pathogenesis. As shown in the heat map presented in figure 4.7, P-I-P-treated mice showed an early upregulation of CCL2, CCL3, CXCL2, CXCL1, and CXCL10 mRNA levels on day 0 p.i. compared to the PBS-treated animals. The normalized fold-change of chemokine mRNAs ranged from 4.45 to 100.08 on day 0 p.i. During the next two time points following PVM infection, CCL3, CXCL2 and CXCL1 mRNA expression remained fairly stable and did not change over time. CCL2 and CXCL10 mRNA levels decreased on day 3 ($p=0.0079$) followed by an increase on day 5 ($p=0.0317$ for CCL2 and $p=0.0159$ for CXCL10). In addition to mRNA, protein levels of CCL2 and CXCL1 were measured in lung homogenate samples. In both P-I-P- and PBS-treated groups, CCL2 and CXCL1 mRNA and protein levels followed a very similar pattern (Figs. 4.8A to 4.8D). PBS-treated mice expressed increasing amounts of these two chemokines over time ($p=0.0079$). The gradual changes in mRNA levels started with a 19- and 29-fold increase on day 3 p.i. for CCL2 and CXCL1, respectively, escalating to a further 17-fold increase for CCL2 and 2-fold increase for CXCL1 on day 5 p.i. In these mice the CCL2 and CXCL1 protein amounts increased dramatically, from 58.2 and 94.0 pg/ml on day 0 p.i. to the staggering amounts of 15,278 and 5,244 pg/ml on day 5 p.i., respectively. In contrast, P-I-P-treated mice not only started with early upregulated

mRNA levels on day 0 p.i., but this expression also remained stable over time being significantly lower than the amounts detected in their PBS-treated animals on day 5 p.i. (Figs. 4.8A, 4.8C). CCL2 and CXCL1 protein concentrations were ~36-fold higher in these mice than in the PBS-treated group on day 0 p.i., On day 5 p.i., CCL2 and CXCL1 protein levels in P-I-P treated animals were 92% and 78% lower than those detected in the PBS-treated group (Figs. 4.8B, 4.8D).

In terms of cytokine molecules, on day 0 p.i., TNF-α, IL-1β, IL-6, IL-12 and IL-10 mRNA were slightly upregulated in the P-I-P-treated group, with highest normalized fold-change of 12.36. On days 3 and 5 p.i., these animals had relatively stable mRNA levels, with normalized-fold changes under 10-fold for most genes (Fig. 4.7). IL-10 was the exception, as on day 5 p.i. mRNA levels were much higher than any other value observed in this group. In the case of TGF-β, mRNA levels did not change over time and were similar to those of the reference gene in both PBS- and P-I-P-treated animals. Regarding the PBS-treated group, the cytokines followed the same trend as the chemokines, characterized by increasing mRNA levels overtime and highest expression on day 5 p.i. This applied to all molecules including IL-10.

	PBS/PVM			P-I-P/PVM		
	Day 0 p.i.	**Day 3 p.i.**	**Day 5 p.i.**	**Day 0 p.i.**	**Day 3 p.i.**	**Day 5 p.i.**
CCL2	1.49	28.21	471.14	39.60	15.43	30.70
CCL3	1.37	5.34	25.56	4.67	6.99	9.69
CXCL2	1.56	24.83	145.61	4.45	7.7	6.22
CXCL1	1.01	29.04	70.82	15.30	10.85	11.36
CXCL10	0.87	64.45	1661.19	100.08	22.63	73.93
TNF-α	0.75	5.99	19.35	7.5	5.7	8.36
IL-1β	1.36	1.49	7.47	4.09	1.77	3.51
IL-6	1.57	21.50	316.93	12.36	6.35	9.18
IL-12β (p40)	0.86	2.22	13.20	6.66	4.9	8.41
IL-10	0.86	4.78	50.56	3.57	4.78	36.25
TGF-β	0.97	0.91	0.89	0.69	0.9	0.83
IFN-α	1.08	23.59	7.72	19.19	1.13	2.6
IFN-β	1.16	21.08	91.90	109.14	6.22	10.50
IFN-γ	0.97	4.73	24.59	3.9	5.51	10.48

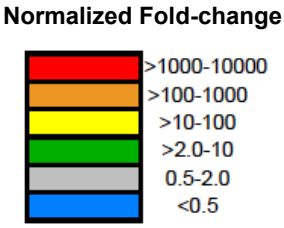

Figure 4.7: Heat map of chemokine and cytokine mRNA expression profiles of 5-6 week-old P-I-P- or PBS-treated Balb/c mice before and after intranasal PVM challenge. Mice were given an intranasal treatment of PBS or P-I-P 24 hr before challenge with 3000 pfu PVM. The single-lobed lungs of 5 mice per group per time point were collected on days 0, 3 and 5 p.i. All Ct values were normalized against the average of the β-actin levels of control animals for each specific time point indicated above. Normalized fold-change calculations were performed using the $2^{-\Delta\Delta Ct}$ method. Data are shown as the median of five biological replicates.

Protein expression trends for TNF-α and IL-6 were similar to their mRNA trends for both P-I-P-and PBS-treated groups (Figs. 4.8F, 4.8J). P-I-P-treated animals displayed 10- and 35-fold higher concentrations of TNF-α and IL-6 proteins, respectively, on day 0 when compared to PBS-treated mice. TNF-α protein concentrations remained relatively constant overtime and IL-6 protein levels decreased by 94% on day 3 p.i. ($p=0.0159$). In contrast, PBS-treated mice had elevated TNF-α and IL-6 protein concentrations on day 5 p.i., which were 57- and 83-fold higher than values in the P-I-P-treated group, respectively. The remaining cytokines assayed displayed a different trend. Although both IL-1β mRNA and protein levels were relatively low in PBS-treated mice, IL-1β mRNA levels remained stable between days 0 and 3 p.i. and protein levels began to rise significantly after day 0 p.i. ($p=0.0079$). P-I-P-treated mice displayed the characteristic early expression of mRNA and protein, which was followed by a constant maintenance of IL-1β levels throughout the 5 days of infection (Figs. 4.8G, 4.8H). The IL-12 p70 protein concentration in PBS-treated mice started to rise between days 3 and 5 p.i. and was significantly higher by day 5 after infection ($p=0.0079$). P-I-P-treated mice had 3X the concentration of IL-12 p70 in PBS-treated animals on day 0 p.i. By day 5 p.i., the former mice had a 92% lower concentration of IL-12 p70 than that measured in the latter group (Figs. 4.8K, 4.8L). Lastly, in PBS-treated mice, IL-10 mRNA levels increased significantly over time ($p=0.0079$), with highest expression on day 5 p.i. The protein concentrations in the lungs began to rise on day 3 p.i., and became significantly higher by day 5 p.i. ($p=0.0079$). In P-I-P-treated mice, mRNA and protein levels started with an early upregulation on day 0 p.i., remained constant till day 3 p.i., and then increased by day 5 after PVM infection ($p=0.0079$). Overall, by day 5 p.i., the levels of most cytokine

molecules in the P-I-P-treated group were significantly lower than those of the PBS-treated group. The exceptions to this trend were IL-1β and IL-10, where protein levels were not significantly different from those of the PBS-treated group.

In terms of the IFN response, P-I-P-treated animals displayed an earlier expression of type I IFN mRNA compared to PBS-treated mice (Fig. 4.7). By day 3 p.i., these mice experienced a significant drop in IFN-α and IFN-β mRNA levels ($p=0.0079$), which then remained constant between days 3 and 5 p.i. In contrast, the PBS-treated animals showed increased expression of type I IFNs throughout the infection. Both IFN-γ mRNA and protein expression were elevated on day 0 in P-I-P-treated mice and were significantly higher than those of the PBS-treated animals (Figs. 4.7, 4.8O, and 4.8P). The PBS-treated mice produced increasing amounts of IFN-γ throughout the infection, especially on day 5 p.i., when both IFN-γ mRNA and protein levels were higher than those in the P-I-P-treated animals (Figs. 4.8O, 4.8P). Overall, these data suggest that P-I-P acts as an immunomodulator capable of preventing chemokine and cytokine molecules from reaching exacerbated levels in the lungs during lethal PVM infection.

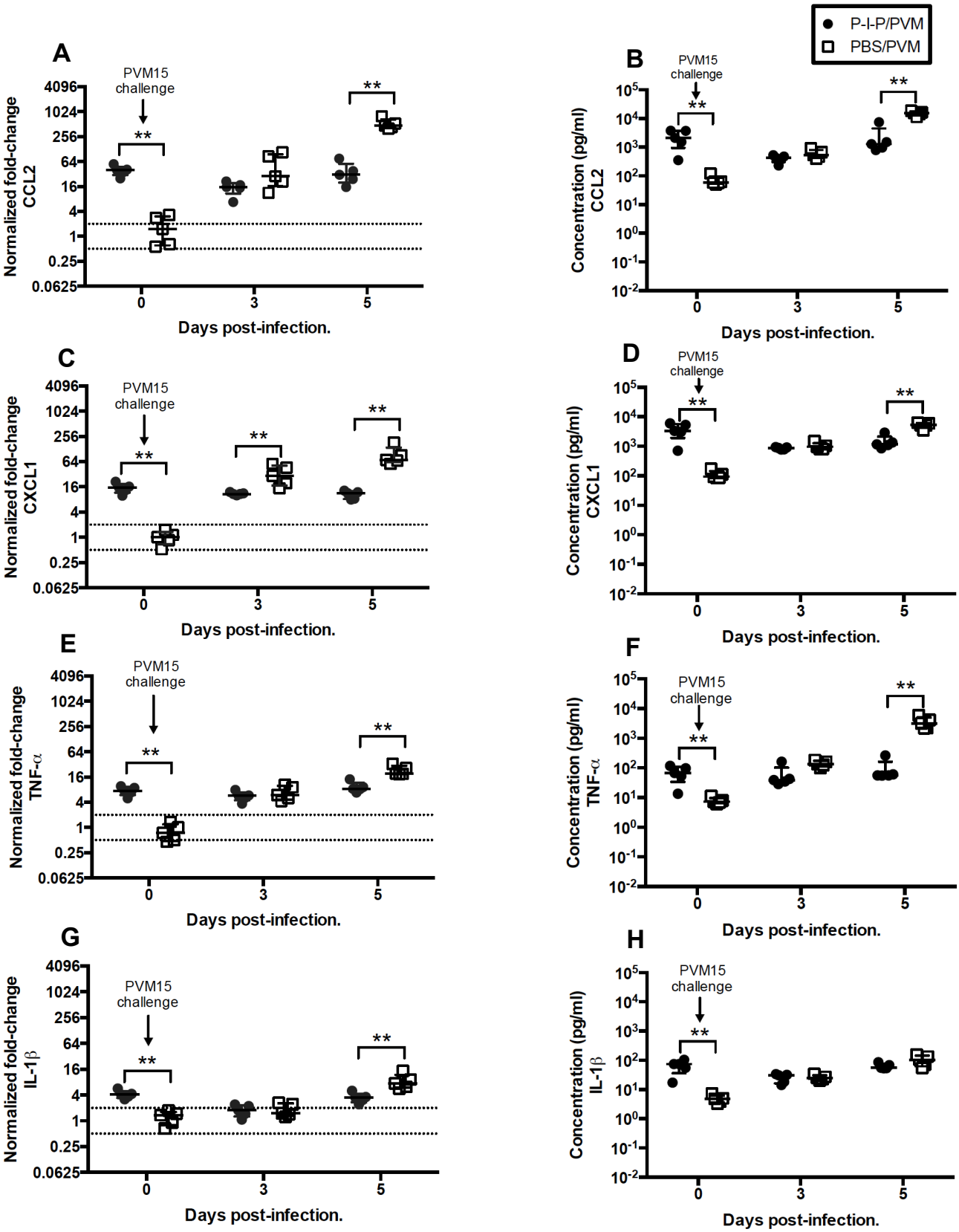
A
PVM15 challenge
**
**
Normalized fold-change CCL2
4096
1024
256
64
16
4
1
0.25
0.0625
0
3
5
Days post-infection.
B
P-I-P/PVM
PBS/PVM
PVM15 challenge
**
**
Concentration (pg/ml) CCL2
10^5
10^4
10^3
10^2
10^1
10^0
10^{-1}
10^{-2}
0
3
5
Days post-infection.
C
PVM15 challenge
**
**
**
Normalized fold-change CXCL1
4096
1024
256
64
16
4
1
0.25
0.0625
0
3
5
Days post-infection.
D
PVM15 challenge
**
**
Concentration (pg/ml) CXCL1
10^5
10^4
10^3
10^2
10^1
10^0
10^{-1}
10^{-2}
0
3
5
Days post-infection.
E
PVM15 challenge
**
**
Normalized fold-change TNF-α
4096
1024
256
64
16
4
1
0.25
0.0625
0
3
5
Days post-infection.
F
PVM15 challenge
**
**
Concentration (pg/ml) TNF-α
10^5
10^4
10^3
10^2
10^1
10^0
10^{-1}
10^{-2}
0
3
5
Days post-infection.
G
PVM15 challenge
**
**
Normalized fold-change IL-1β
4096
1024
256
64
16
4
1
0.25
0.0625
0
3
5
Days post-infection.
H
PVM15 challenge
**
Concentration (pg/ml) IL-1β
10^5
10^4
10^3
10^2
10^1
10^0
10^{-1}
10^{-2}
0
3
5
Days post-infection.

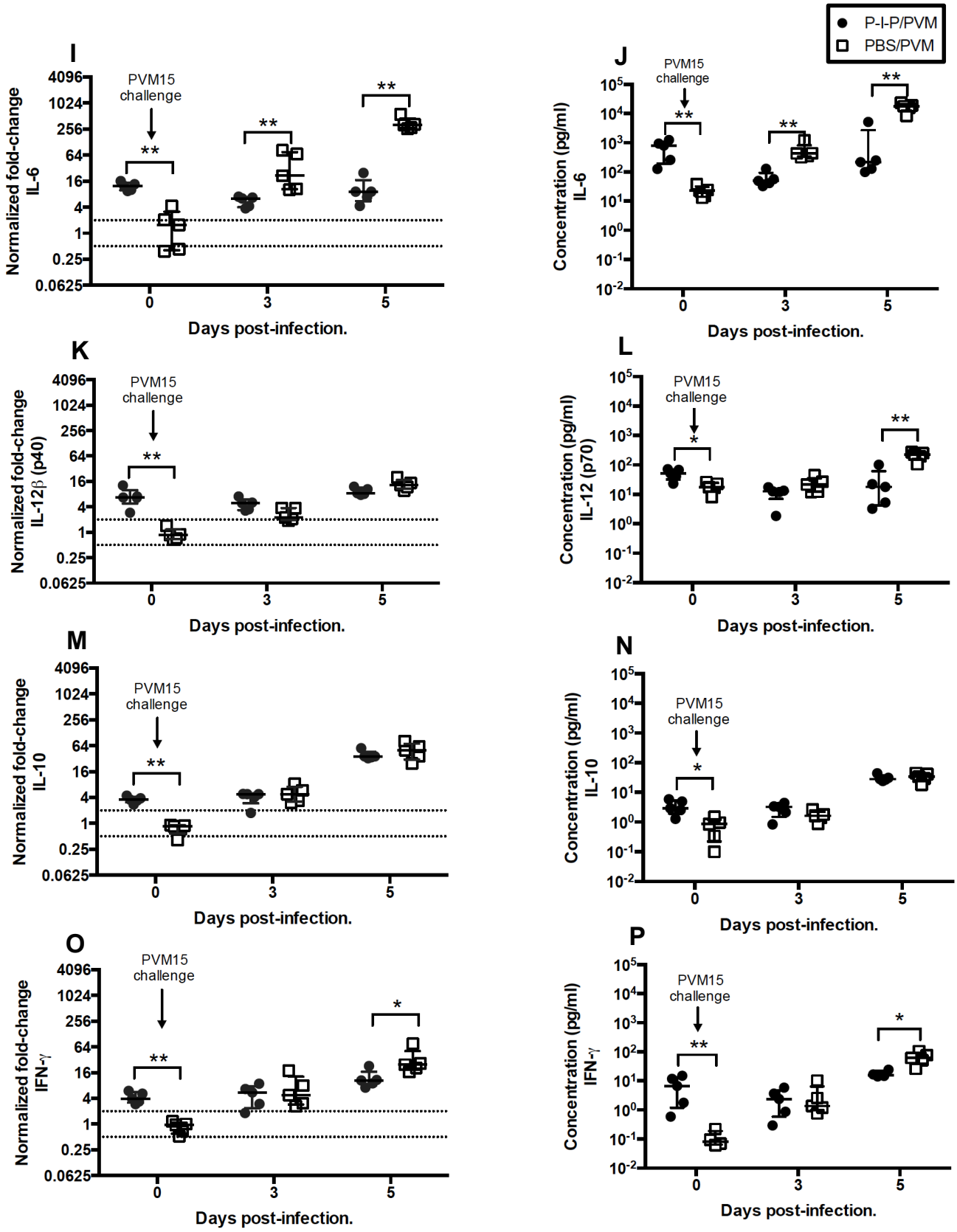
I
Normalized fold-change IL-6
PVM15 challenge
Days post-infection.
J
P-I-P/PVM
PBS/PVM
Concentration (pg/ml) IL-6
K
Normalized fold-change IL-12β (p40)
L
Concentration (pg/ml) IL-12 (p70)
M
Normalized fold-change IL-10
N
Concentration (pg/ml) IL-10
O
Normalized fold-change IFN-γ
P
Concentration (pg/ml) IFN-γ

Figure 4.8: Comparison between lung mRNA and protein expression levels of chemokine and cytokine genes of P-I-P pre-treated Balb/c mice. Mice were given an intranasal treatment of PBS or P-I-P 24 hr before challenge with 3000 pfu PVM. The single- and multi-lobed lungs of 5 mice per group per time point were collected separately for each individual animal on days 0, 3 and 5 p.i. Gene expression was assayed by qPCR, and protein expression by electrochemiluminescence-based multiplex ELISAs. Panels A, C, E, G, I, K, M, and O represent mRNA expression of CCL2, CXCL1, TNF-α, IL-1β, IL-6, IL-12β (p40), IL-10, and IFN-γ, respectively. All Ct values were normalized against the average of the β-actin levels of control animals for each specific time point indicated above. Normalized fold-change calculations were performed using the $2^{-\Delta\Delta Ct}$ method. Two horizontal dotted lines at 0.5- and 2-fold were generated to indicate downregulation and upregulation respectively. Panels B, D, F, H, J, L, N and P represent protein expression data in pg/mL for CCL2, CXCL1, TNF-α, IL-1β, IL-6, total IL-12 (p70), IL-10, and IFN-γ, respectively. Data are shown as individual values representing single animals as well as median with interquartile range of five biological replicates. Only statistically significant differences are indicated in the plots. *$p<0.05$ and **$p<0.01$.

4.5. Weight loss and mortality increases when P-I-P treatment is delivered at earlier time points prior to infection.

With a better understanding of P-I-P's mechanism of action in terms of innate immunity, we decided to further investigate the duration of protection that P-I-P is capable of conferring to mice from lethal PVM challenge. For these experiments, we followed the same protocols as before, but instead of delivering the treatment 24 hr prior to challenge, we treated mice with P-I-P at 3, 4, 5 or 6 days prior to PVM infection. Weights and clinical signs were monitored throughout the entire trial, including the days following treatment. In certain experiments we collected lungs of survivor mice on day 14 p.i. to measure PVM copy numbers and determine if these mice were PVM-negative using qPCR. Animals treated 3 days prior to infection experienced weight loss of less than 10% and survival of 90% (Figs. 4.9A, 4.9B). Also, these mice had low scores for weight loss and appearance (Figs. 4.10A, 4.10B). When P-I-P treatment was delivered 4 days prior to challenge, mice had a further increase in weight loss (i.e. between 10-12%) and a survival rate of 60% (Figs. 4.9C, 4.9D). Clinical scores for weight changes and appearance also increased slightly (Figs. 4.10C, 4.10D). Mice that received P-I-P treatment on day -5 had a weight loss greater than 15%, a survival rate of 50% (Figs. 4.9E, 4.9F) and more severe clinical signs (Figs. 4.10E, 4.9F). Lastly, mice with P-I-P treatment delivered on day -6 showed weight loss of 20% and survival of 30% (Figs. 4.9G, 4.9H). Clinical scores were higher, both weight loss and appearance with highest scores of 2 (Figs. 4.10G, 4.10H). This trend suggests that treatment efficacy is reduced the earlier the treatment is delivered, leading to a poorer performance at providing

protection against severe PVM disease. We noted that P-I-P still had good activity up to 3 days prior to infection. However, when administered on day -4 or earlier, the effect of P-I-P started to lose potency resulting in less favorable clinical outcomes overall. Regardless of the setting and day of the treatment, survivor mice of the day -3 and -6 trials were PVM-negative on day 14 p.i., suggesting that P-I-P pre-treatment is able to mediate complete clearance of PVM from the lungs of survivors.

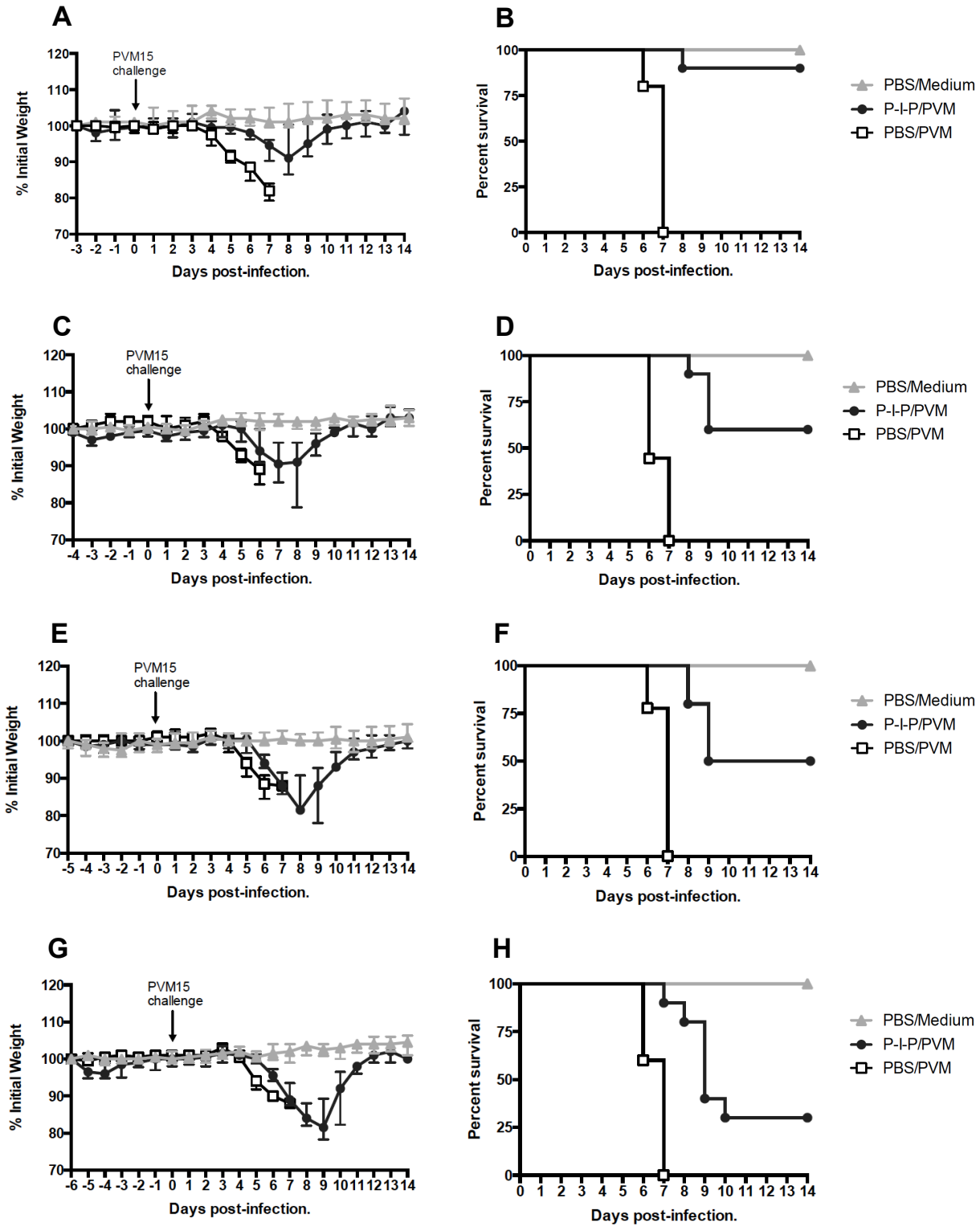
A
PVM15 challenge
% Initial Weight
Days post-infection.
B
Percent survival
Days post-infection.
PBS/Medium
P-I-P/PVM
PBS/PVM
C
PVM15 challenge
% Initial Weight
Days post-infection.
D
Percent survival
Days post-infection.
PBS/Medium
P-I-P/PVM
PBS/PVM
E
PVM15 challenge
% Initial Weight
Days post-infection.
F
Percent survival
Days post-infection.
PBS/Medium
P-I-P/PVM
PBS/PVM
G
PVM15 challenge
% Initial Weight
Days post-infection.
H
Percent survival
Days post-infection.
PBS/Medium
P-I-P/PVM
PBS/PVM

Figure 4.9: Percent weight loss and survival scores of Balb/c mice treated with P-I-P or PBS 3, 4, 5 and 6 days prior to intranasal PVM challenge. Mice were given prophylactic intranasal treatment of PBS or P-I-P at the time points indicated above, followed by a 3000 pfu PVM challenge. Animals were weighed and scored daily after treatment and for 14 days following infection. Panels A, C, E, and G show weight loss of mice treated 3, 4, 5 and 6 days prior to PVM infection, respectively, expressed as the median percentage of the starting weight with error bars indicating the interquartile range. Panels B, D, F and H illustrate percent survival of mice treated 3, 4, 5 and 6 days prior to infection, respectively, expressed as the median percentage of the total number of animals per group during the 14 days following infection. Each experiment was performed twice and all graphs illustrate the combined results of these two experiments. The total number of animals equals to 10 per group, with an n = 5 for each experiment.

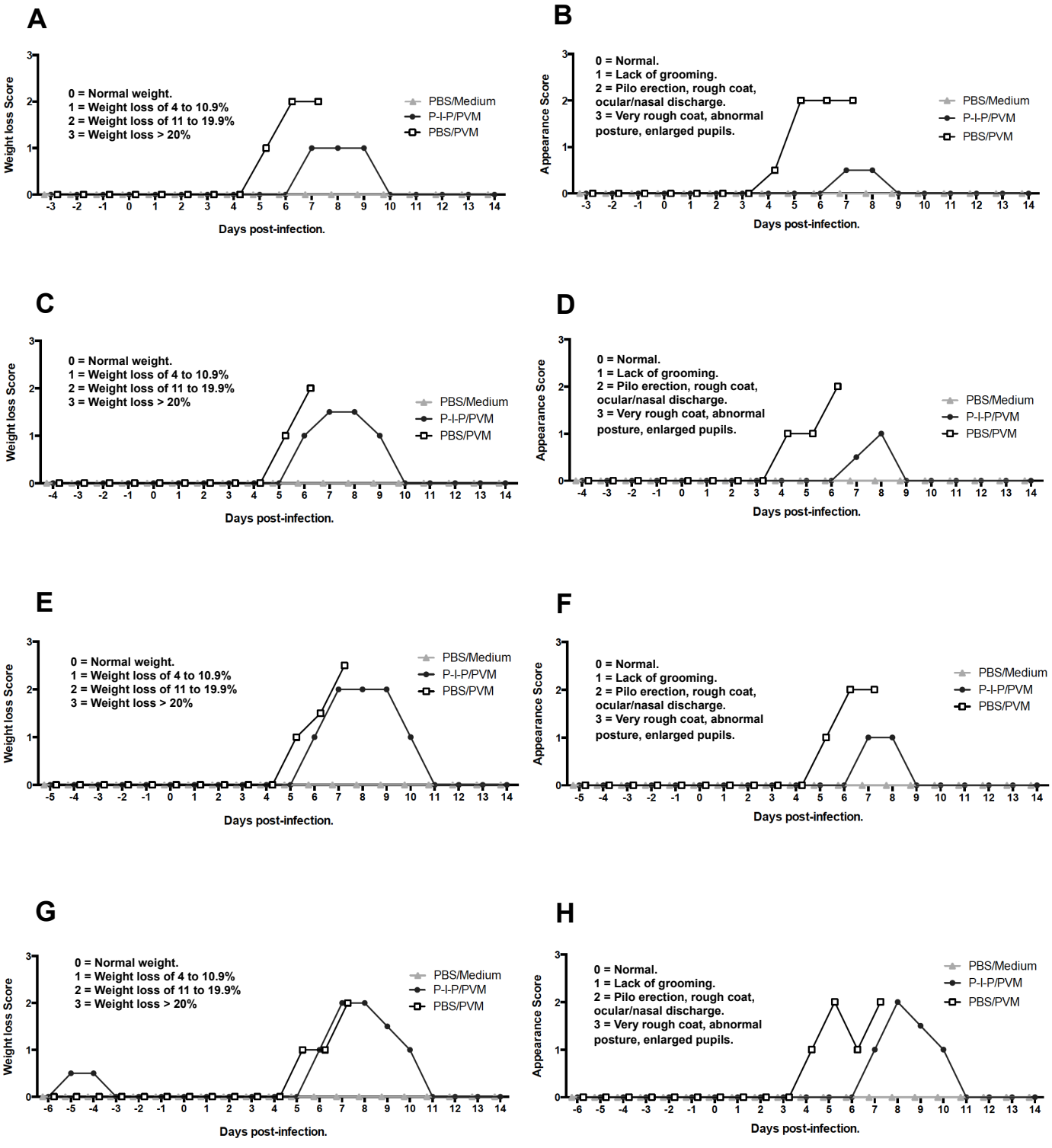
A
Weight loss Score
0 = Normal weight.
1 = Weight loss of 4 to 10.9%
2 = Weight loss of 11 to 19.9%
3 = Weight loss > 20%
PBS/Medium
P-I-P/PVM
PBS/PVM
Days post-infection.
B
Appearance Score
0 = Normal.
1 = Lack of grooming.
2 = Pilo erection, rough coat, ocular/nasal discharge.
3 = Very rough coat, abnormal posture, enlarged pupils.
PBS/Medium
P-I-P/PVM
PBS/PVM
Days post-infection.
C
Weight loss Score
0 = Normal weight.
1 = Weight loss of 4 to 10.9%
2 = Weight loss of 11 to 19.9%
3 = Weight loss > 20%
PBS/Medium
P-I-P/PVM
PBS/PVM
Days post-infection.
D
Appearance Score
0 = Normal.
1 = Lack of grooming.
2 = Pilo erection, rough coat, ocular/nasal discharge.
3 = Very rough coat, abnormal posture, enlarged pupils.
PBS/Medium
P-I-P/PVM
PBS/PVM
Days post-infection.
E
Weight loss Score
0 = Normal weight.
1 = Weight loss of 4 to 10.9%
2 = Weight loss of 11 to 19.9%
3 = Weight loss > 20%
PBS/Medium
P-I-P/PVM
PBS/PVM
Days post-infection.
F
Appearance Score
0 = Normal.
1 = Lack of grooming.
2 = Pilo erection, rough coat, ocular/nasal discharge.
3 = Very rough coat, abnormal posture, enlarged pupils.
PBS/Medium
P-I-P/PVM
PBS/PVM
Days post-infection.
G
Weight loss Score
0 = Normal weight.
1 = Weight loss of 4 to 10.9%
2 = Weight loss of 11 to 19.9%
3 = Weight loss > 20%
PBS/Medium
P-I-P/PVM
PBS/PVM
Days post-infection.
H
Appearance Score
0 = Normal.
1 = Lack of grooming.
2 = Pilo erection, rough coat, ocular/nasal discharge.
3 = Very rough coat, abnormal posture, enlarged pupils.
PBS/Medium
P-I-P/PVM
PBS/PVM
Days post-infection.

Figure 4.10: Clinical scores of Balb/c mice treated with P-I-P or PBS 3, 4, 5 and 6 days prior to intranasal PVM challenge. Mice were given prophylactic intranasal treatment of PBS or P-I-P on the time points indicated above, followed by a 3000 pfu PVM challenge. Animals were weighed and scored daily after treatment and for 14 days following infection. Panels A, C, E and G represent clinical score for weight loss and panels B, D, F and H illustrate clinical scores for changes in appearance of mice treated 3, 4, 5 and 6 days prior to lethal PVM infection, respectively. Data are presented as the median value for each group during the entirety of the animal trial. Each experiment was performed twice and all graphs illustrate the combined results of the two sets of experiments. The total number of animals equals to 10 per group, with an n = 5 for each experiment.

5. DISCUSSION AND CONCLUSIONS

5.1. Immunomodulators in the context of microbial infections.

Most immunomodulatory regimes for infectious diseases have two major goals: enhance pathogen clearance and suppress undesirable immune responses. Examples of these can be found in the context of both bacterial and viral infections. IFN-γ in conjunction with gentamicin or vancomycin is effective at reducing morbidity and mortality against drug-resistant *Enterococcus faecalis* in mice [122]. Administration of CpG ODN protects specific-pathogen-free mice against *Listeria monocytogenes* and *Francisella tularensis* [123]. Similarly, treatment with various immunomodulators for prophylaxis has been previously performed in both influenza and Severe Acute Respiratory Syndrome coronavirus (SARS-CoV) infection models [108, 124]. With regards to PVM as well as RSV, an effective therapeutic approach should be both antiviral and immunomodulatory in nature [12, 125]. One group demonstrated this principle for PVM by injecting mice with ribavirin together with CCL3 blockade by either gene-deletion or antibody [125]. The overall conclusion of their study was that it is in fact required to have both antiviral and immunomodulatory components in a treatment regimen against PVM. The group found that in order to achieve the desired outcomes, two daily doses of ribavirin and a single daily dose of anti-CCL3 antibody were required during a period of 12 days [125]. As mentioned in the introduction, ribavirin is known to induce toxicity and severe side effects in pediatric patients, discouraging its use in these populations. A few advantages of P-I-P treatment include the fact that it indirectly

induces moderate antiviral activity and also possess the ability to down-modulate levels of chemokines like CCL3 during PVM infection. This was also the case for other biological mediators of disease pathogenesis such as CCL2, involved in monocyte recruitment, CXCL1, key mediator of neutrophil chemotaxis, as well as TNF-α and IL-6, which induce vascular permeability and activation of high endothelial venules. If delivered 24 hr prior to PVM infection, P-I-P leads to the effective clearance of the virus, in conjunction with excellent survival rates, minimal clinical disease and no short-term observable side effects.

5.2. The importance of well-regulated innate immune responses in the control of viral respiratory infections.

Alveolar macrophages are pivotal patrollers of the lung milieu whose major role is to maintain homeostasis within this tissue [126, 127]. In the context of respiratory viral infections, it has been reported that alveolar macrophages, in conjunction to pDCs, are key mediators of viral clearance and disease resolution *in vivo* [128, 129]. One group has recently shown that depletion of alveolar macrophages by intranasal administration of dichloromethylene bisphosphonate liposomes prior to RSV infection resulted in increased virus titers in the lungs, exacerbated disease and lung inflammation within the tissue [129]. P-I-P treatment is associated with enhanced viral clearance, reduced immunopathology as well as higher alveolar macrophage numbers in the lungs during lethal PVM infection. It is likely that the latter event provided P-I-P-treated mice with a

clear advantage, as alveolar macrophages are known to dampen excess inflammatory responses within the lung microenvironment [130].

As reviewed by *Gabelloni et al*., it is suggested that neutrophils may play an important role in the regulation of local immunity, as these cells secrete a multitude of molecules that modify immune responses [131]. One study showed that uncontrolled influx of neutrophils during an active influenza infection leads to severe lung inflammation [132, 133]. Similarly, prominent granulocyte accumulation in the lungs is a hallmark of PVM infection, which eventually progresses to pulmonary edema and respiratory distress [134]. In contrast, one group showed that mice depleted of neutrophils before the establishment of influenza A virus infection developed increased morbidity and mortality [128, 133]. This evidence suggests that neutrophil infiltration does not always lead to detrimental outcomes as it was once thought to do. Interestingly, early neutrophil influx was detected in P-I-P-treated mice. While it is possible that the treatment itself is able to mediate moderate neutrophil recruitment into the lungs by the production of chemo-attractants like CXCL1 and CXCL2, these mice did not show signs of neutrophilia. Instead, these animals had low neutrophil counts that were maintained at stable levels throughout the days following treatment and infection. Our results are in agreement with the concept that neutrophils are likely to participate in the effective control and clearance of viral pathogens, if and only if these are adequately recruited and regulated within the tissue in a manner that prevents immunopathology from occurring.

Previously, as well as in the current study, we and others showed that NK cell recruitment takes place at later time points during PVM infection [13, 135], which is correlated to an increase in lung virus titers, suggesting that the NK cell recruitment

occurs too late to be beneficial. It is likely that P-I-P pre-treatment has a direct effect on NK cell biology. P-I-P induced the production of chemokines involved in NK cell recruitment, namely CCL2, CCL3 and CXCL10. Thus, this cell population infiltrated the lungs much earlier than it normally would during a natural PVM infection. In addition, P-I-P pre-treatment induced the production of cytokines involved in NK cell activation, such as IFN-β and IL-12. Therefore, it is possible to assume that P-I-P-treated mice have an effective local antiviral innate immune response prior to the establishment of an active PVM infection within the airways of these animals.

Type I IFN mRNA was upregulated shortly after P-I-P intranasal delivery. If these molecules are present in the lungs prior to infection, they can promote an antiviral state required to limit virus replication in both infected and bystander cells [136]. Perhaps this is another mechanism contributing to the reduction in PVM titers observed on days 3 and 5 p.i.

5.3. Advantages of P-I-P as an alternative approach to treat RSV infections in susceptible populations.

The attractiveness of P-I-P as an immunomodulator is due to the complementary properties of its individual constituents. Poly I:C is a PRR ligand with immunostimulatory activity, especially in applications involving cancer immunotherapies, and more recently in treatment against infectious diseases and as vaccine adjuvants [102, 108, 137]. Poly I:C signals through PRRs such as TLR3, RIG-I and MDA-5. It induces the production of pro-inflammatory cytokines, chemokines and

type I IFNs. The latter is of great importance as most paramyxoviruses inhibit IFN-α/β through the NS1/NS2 proteins [13]. However, as mentioned previously, too much stimulation of local immune responses can result in detrimental effects to the organ system in question, in this case the respiratory tract. Due to the nature of poly I:C and its downstream signaling cascade, it has the potential to exacerbate RSV-induced pro-inflammation due to the possible amplification of the NF-κB pathway. We believe that P-I-P has an advantage over poly I:C therapies as it is more modulatory in nature. This property in fact would benefit individuals at risk of RSV infection because it ensures optimal regulation of immune responses in the context of an active infection. Innate defense regulator peptides are able to modulate immune responses *in vivo* by reducing levels of pro-inflammatory mediators, modulate the expression of host defense genes within macrophages and other immune cells, and are able to selectively recruit innate immune cells into the site of infection [113]. Most studies involving IDR peptides as immunomodulators focus on bacterial pathogens [113]. We believe that IDR peptide 1002 is one of the major anti-inflammatory components in our formulation as it has been previously shown that other peptides of its kind are able to selectively suppress downstream signaling events in response to different TLR agonists [113]. Lastly, PCEP is a polyphosphazene of synthetic origin known for its immunoadjuvant activity and as a delivery vehicle. This is the first study of its kind using PCEP in an immunomodulatory treatment formulation rather than as an adjuvant.

We propose that P-I-P can be used prophylactically for the prevention of RSV infections in high-risk populations like young children and the elderly. These populations possess immune systems that do not perform optimally, due either to immune immaturity

or senescence. Thus, it is quite logical to use immunostimulatory compounds to enhance host immune responses to combat viral infections. Furthermore, P-I-P as an immunotherapy against RSV would be more cost-effective than monoclonal antibody, which is currently used as prophylaxis in high-risk infants. Up to 3 days prior to exposure, P-I-P protected approximately 90% of the animals. If P-I-P were to be taken regularly, for instance every 3 days, one might maintain a longer protective state in the respiratory tract. The local and systemic effects of taking a steady P-I-P regimen are yet to be elucidated. This concept is particularly attractive for the elderly. Taking into consideration that RSV infections are most predominant in fall and winter seasons, elderly patients inhabiting nursing homes could be treated with the P-I-P formulation during outbreaks of RSV or possibly other respiratory infections such that partial immune protection can be provided. The lack of antigen in our formulation suggests that P-I-P acts primarily at the level of the innate immune system of the host. This fact allows us to speculate on the possibility of a well-established P-I-P therapy to protect patients from multiple viral infections at once. It would be beneficial if one can protect the most vulnerable populations from major diseases like influenza, CoV, and RSV infections as most of these tend to be transmitted through the same route of exposure and during the same seasons. However, studies confirming such pleiotropic effect are yet to be performed.

We used a lethal dose of PVM in all our animal studies as a disease model in order to provide a proof of concept for the effectiveness of P-I-P. In the context of RSV infections, it is unlikely that one would be naturally exposed to such doses of virus inoculum. When used in a real-life scenario, as a treatment against RSV, P-I-P

prophylaxis might last much longer than what we reported using the PVM disease model. If the viral challenge dose were reduced, we would probably obtain more survivors as a result of P-I-P administration at earlier time points before PVM challenge. The downside of such an approach is that it would be unclear if any reduction in virus replication and disease were due to the direct effect of P-I-P or the sub-lethal nature of the challenge itself. Nonetheless, studies involving a lower virus challenge might be required as these are likely to complement the existing data with information regarding the nature of both innate and adaptive immune responses during a full course of PVM infection. In this way, we would be able to mimic a more realistic setting of infection resulting in a better understanding of the potential effects of P-I-P in humans.

5.4. General conclusions and future directions.

In the present study we assessed the potential of a novel immunomodulatory treatment, P-I-P, in a PVM disease model as an alternative approach to treat severe respiratory infections. A single dose of P-I-P significantly upregulated the expression of genes involved in host defense as early as 6 hr p.t. Most cytokines and chemokines remained at fairly high levels from 6 to 24 hr p.t. Thereafter, these levels decreased as expected due to their relatively short half-lives. These data suggested that 24 hr prior to challenge would be an ideal starting time point for the initial delivery of P-I-P as a treatment against lethal PVM disease. Treatment at 24 hr prior to PVM challenge reduced weight loss, clinical symptoms and lung immunopathology, and conferred complete survival. P-I-P displayed genuine immunomodulating potential as it stimulated early

expression of key chemokines and cytokines involved in PVM pathogenesis and host defense; it also downregulated the levels of such factors during the first 5 days following PVM infection. It is important to highlight the fact that P-I-P did not cause any short-term observable adverse effects as evidenced by the absence of clinical signs following treatment. Another important feature of P-I-P immunomodulation is the substantial reduction of neutrophil and eosinophil influx during infection. Interestingly, P-I-P mediated early recruitment of NK cells and DCs into the lungs. Influx of alveolar macrophages was also increased, but its peak took place on day 3 p.i. Lastly, the protective effect of P-I-P was maintained if delivered as early as 3 days prior to lethal challenge. It is worth mentioning that survivor mice were deemed PVM-free on day 14 p.i. This suggests that P-I-P modulation of host immune responses is able to trigger complete clearance of the virus from the site of infection.

As mentioned previously, the flexible nature of P-I-P as an immunomodulator allows for its potential use as an immunotherapy against other infectious diseases. We would like to try this approach against other infectious agents, starting with other respiratory viruses, moving to bacterial respiratory diseases, and so on. In order to do this, a thorough understanding of its mechanism of action is required. We believe that P-I-P prophylaxis can condition the respiratory tract of the animals with a controlled inflammatory innate immune response. This, in turn, would alter the virus life cycle, preventing it from thriving and causing a dysfunctional and exacerbated inflammatory syndrome. For future studies, it would be very interesting to use knockout mice or perform immune cell depletions *in vivo,* as it is likely that both cellular and soluble factors play a major role in the mechanism of protection mediated by P-I-P. It may be of

interest to investigate the role of early recruited neutrophils in P-I-P treated mice by administering antibodies intravenously to deplete these granulocytes temporarily. In this way, it could provide us with important evidence regarding the direct contribution of neutrophils into the main mechanism of action of our formulation. Additionally, other studies should focus on cells that promote antiviral immunity in the airways such as NK cells, alveolar macrophages, interstitial macrophages and pDCs. Monocyte infiltration into the lungs was not investigated in detail during this study, but based on the overall chemokine profile detected during P-I-P treatment and PVM infection, we can speculate that monocytes are certainly being recruited into the site of infection (i.e. high expression of CCL2). It would be worthwhile to study this cell population as monocytes may directly contribute to viral clearance within the tissue as well as the development of immunopathology [138]. *Stat1*$^{-/-}$ or *Ifnar*$^{-/-}$ gene knockout experiments could be performed to validate the direct contribution of P-I-P-induced IFNs in mediating protection against lethal PVM disease *in vivo*. A common feature of many RSV surrogate animal models is the fact that age seems to have a direct influence in disease susceptibility. Thus, it would be worthwhile to study the protective effects of P-I-P in different age groups (i.e. neonates, elderly). Lastly, we would like to explore P-I-P as a therapeutic agent by adjusting the relative dose of P-I-P and its individual constituents as well as the number of intranasal treatments needed that is most suitable for such an application. In that way, we can propose an optimum treatment course that is suitable for different types of respiratory disease severities and susceptibilities.

(Manuscript to be submitted to Antiviral Research.)

6. REFERENCES

1. Graham, B.S. and L.J. Anderson, *Challenges and opportunities for respiratory syncytial virus vaccines.* Curr Top Microbiol Immunol, 2013. **372**: p. 391-404.
2. Chanock, R.M., et al., *Acute respiratory diseases of viral etiology. IV. Respiratory syncytial virus.* Am J Public Health Nations Health, 1962. **52**: p. 918-25.
3. Chanock, R., B. Roizman, and R. Myers, *Recovery from infants with respiratory illness of a virus related to chimpanzee coryza agent (CCA). I. Isolation, properties and characterization.* Am J Hyg, 1957. **66**(3): p. 281-90.
4. Prober, C.G. and W.M. Sullender, *Advances in prevention of respiratory syncytial virus infections.* J Pediatr, 1999. **135**(5): p. 546-58.
5. Garg, R., P. Shrivastava, and S. van Drunen Littel-van den Hurk, *The role of dendritic cells in innate and adaptive immunity to respiratory syncytial virus, and implications for vaccine development.* Expert Rev Vaccines, 2012. **11**(12): p. 1441-57.
6. Borchers, A.T., et al., *Respiratory syncytial virus--a comprehensive review.* Clin Rev Allergy Immunol, 2013. **45**(3): p. 331-79.
7. Papadopoulos, N.G., et al., *Does respiratory syncytial virus subtype influences the severity of acute bronchiolitis in hospitalized infants?* Respir Med, 2004. **98**(9): p. 879-82.
8. McNamara, P.S. and R.L. Smyth, *The pathogenesis of respiratory syncytial virus disease in childhood.* Br Med Bull, 2002. **61**: p. 13-28.
9. Hurwitz, J.L., *Respiratory syncytial virus vaccine development.* Expert Rev Vaccines, 2011. **10**(10): p. 1415-33.
10. Dudas, R.A. and R.A. Karron, *Respiratory syncytial virus vaccines.* Clin Microbiol Rev, 1998. **11**(3): p. 430-9.
11. Shaw, C.A., et al., *The path to an RSV vaccine.* Curr Opin Virol, 2013. **3**(3): p. 332-42.

12. Rosenberg, H.F., et al., *The pneumonia virus of mice infection model for severe respiratory syncytial virus infection: identifying novel targets for therapeutic intervention.* Pharmacol Ther, 2005. **105**(1): p. 1-6.
13. Watkiss, E.R., et al., *Innate and adaptive immune response to pneumonia virus of mice in a resistant and a susceptible mouse strain.* Viruses, 2013. **5**(1): p. 295-320.
14. Stockman, L.J., et al., *Respiratory syncytial virus-associated hospitalizations among infants and young children in the United States, 1997-2006.* Pediatr Infect Dis J, 2012. **31**(1): p. 5-9.
15. van Gageldonk-Lafeber, A.B., et al., *A case-control study of acute respiratory tract infection in general practice patients in The Netherlands.* Clin Infect Dis, 2005. **41**(4): p. 490-7.
16. Fjaerli, H.O., T. Farstad, and D. Bratlid, *Hospitalisations for respiratory syncytial virus bronchiolitis in Akershus, Norway, 1993-2000: a population-based retrospective study.* BMC Pediatr, 2004. **4**(1): p. 25.
17. Leader, S. and K. Kohlhase, *Recent trends in severe respiratory syncytial virus (RSV) among US infants, 1997 to 2000.* J Pediatr, 2003. **143**(5 Suppl): p. S127-32.
18. Jansen, A.G., et al., *Influenza- and respiratory syncytial virus-associated mortality and hospitalisations.* Eur Respir J, 2007. **30**(6): p. 1158-66.
19. Mullooly, J.P., et al., *Influenza- and RSV-associated hospitalizations among adults.* Vaccine, 2007. **25**(5): p. 846-55.
20. Falsey, A.R., et al., *Respiratory syncytial virus infection in elderly and high-risk adults.* N Engl J Med, 2005. **352**(17): p. 1749-59.
21. Nair, H., et al., *Global burden of acute lower respiratory infections due to respiratory syncytial virus in young children: a systematic review and meta-analysis.* Lancet, 2010. **375**(9725): p. 1545-55.
22. Nair, H., et al., *Global and regional burden of hospital admissions for severe acute lower respiratory infections in young children in 2010: a systematic analysis.* Lancet, 2013. **381**(9875): p. 1380-90.

23. Kim, H.W., et al., *Respiratory syncytial virus disease in infants despite prior administration of antigenic inactivated vaccine.* Am J Epidemiol, 1969. **89**(4): p. 422-34.

24. Tregoning, J.S. and J. Schwarze, *Respiratory viral infections in infants: causes, clinical symptoms, virology, and immunology.* Clin Microbiol Rev, 2010. **23**(1): p. 74-98.

25. Hammer, J., A. Numa, and C.J. Newth, *Albuterol responsiveness in infants with respiratory failure caused by respiratory syncytial virus infection.* J Pediatr, 1995. **127**(3): p. 485-90.

26. van Woensel, J.B., H. Vyas, and S.T. Group, *Dexamethasone in children mechanically ventilated for lower respiratory tract infection caused by respiratory syncytial virus: a randomized controlled trial.* Crit Care Med, 2011. **39**(7): p. 1779-83.

27. Georgescu, G. and R.F. Chemaly, *Palivizumab: where to from here?* Expert Opin Biol Ther, 2009. **9**(1): p. 139-47.

28. Groothuis, J.R., et al., *Prophylactic administration of respiratory syncytial virus immune globulin to high-risk infants and young children. The Respiratory Syncytial Virus Immune Globulin Study Group.* N Engl J Med, 1993. **329**(21): p. 1524-30.

29. Johnson, S., et al., *Development of a humanized monoclonal antibody (MEDI-493) with potent in vitro and in vivo activity against respiratory syncytial virus.* J Infect Dis, 1997. **176**(5): p. 1215-24.

30. Geskey, J.M., N.J. Thomas, and G.L. Brummel, *Palivizumab: a review of its use in the protection of high risk infants against respiratory syncytial virus (RSV).* Biologics, 2007. **1**(1): p. 33-43.

31. *Palivizumab, a Humanized Respiratory Syncytial Virus Monoclonal Antibody, Reduces Hospitalization From Respiratory Syncytial Virus Infection in High-risk Infants.* Pediatrics, 1998. **102**(3): p. 531-7.

32. Feltes, T.F., et al., *Palivizumab prophylaxis reduces hospitalization due to respiratory syncytial virus in young children with hemodynamically significant congenital heart disease.* J Pediatr, 2003. **143**(4): p. 532-40.

33. Abraha, H.Y., K.L. Lanctot, and B. Paes, *Risk of respiratory syncytial virus infection in preterm infants: reviewing the need for prevention.* Expert Rev Respir Med, 2015. **9**(6): p. 779-99.
34. Wegner, S., et al., *Direct cost analyses of palivizumab treatment in a cohort of at-risk children: evidence from the North Carolina Medicaid Program.* Pediatrics, 2004. **114**(6): p. 1612-9.
35. Eiland, L.S., *Respiratory syncytial virus: diagnosis, treatment and prevention.* J Pediatr Pharmacol Ther, 2009. **14**(2): p. 75-85.
36. Jafri, H.S., *Treatment of respiratory syncytial virus: antiviral therapies.* Pediatr Infect Dis J, 2003. **22**(2 Suppl): p. S89-92; discussion S92-3.
37. Razonable, R.R., *Antiviral drugs for viruses other than human immunodeficiency virus.* Mayo Clin Proc, 2011. **86**(10): p. 1009-26.
38. Ventre, K. and A. Randolph, *Ribavirin for respiratory syncytial virus infection of the lower respiratory tract in infants and young children.* Cochrane Database Syst Rev, 2004(4): p. CD000181.
39. Ghosh, S., et al., *Respiratory syncytial virus upper respiratory tract illnesses in adult blood and marrow transplant recipients: combination therapy with aerosolized ribavirin and intravenous immunoglobulin.* Bone Marrow Transplant, 2000. **25**(7): p. 751-5.
40. Openshaw, P.J. and J.S. Tregoning, *Immune responses and disease enhancement during respiratory syncytial virus infection.* Clin Microbiol Rev, 2005. **18**(3): p. 541-55.
41. Vandini, S., et al., *Immunological, Viral, Environmental, and Individual Factors Modulating Lung Immune Response to Respiratory Syncytial Virus.* Biomed Res Int, 2015. **2015**: p. 875723.
42. Collins, P.L. and B.S. Graham, *Viral and host factors in human respiratory syncytial virus pathogenesis.* J Virol, 2008. **82**(5): p. 2040-55.
43. Bueno, S.M., et al., *Host immunity during RSV pathogenesis.* Int Immunopharmacol, 2008. **8**(10): p. 1320-9.
44. Hacking, D. and J. Hull, *Respiratory syncytial virus--viral biology and the host response.* J Infect, 2002. **45**(1): p. 18-24.

45. Midulla, F., et al., *Respiratory syncytial virus lung infection in infants: immunoregulatory role of infected alveolar macrophages.* J Infect Dis, 1993. **168**(6): p. 1515-9.
46. Kawai, T. and S. Akira, *The role of pattern-recognition receptors in innate immunity: update on Toll-like receptors.* Nat Immunol, 2010. **11**(5): p. 373-84.
47. Rudd, B.D., et al., *Differential role for TLR3 in respiratory syncytial virus-induced chemokine expression.* J Virol, 2005. **79**(6): p. 3350-7.
48. Loo, Y.M., et al., *Distinct RIG-I and MDA5 signaling by RNA viruses in innate immunity.* J Virol, 2008. **82**(1): p. 335-45.
49. Onoguchi, K., et al., *Viral infections activate types I and III interferon genes through a common mechanism.* J Biol Chem, 2007. **282**(10): p. 7576-81.
50. Liu, P., et al., *Retinoic acid-inducible gene I mediates early antiviral response and Toll-like receptor 3 expression in respiratory syncytial virus-infected airway epithelial cells.* J Virol, 2007. **81**(3): p. 1401-11.
51. van Drunen Littel-van den Hurk, S. and E.R. Watkiss, *Pathogenesis of respiratory syncytial virus.* Curr Opin Virol, 2012. **2**(3): p. 300-5.
52. Laham, F.R., et al., *Differential production of inflammatory cytokines in primary infection with human metapneumovirus and with other common respiratory viruses of infancy.* J Infect Dis, 2004. **189**(11): p. 2047-56.
53. Sheeran, P., et al., *Elevated cytokine concentrations in the nasopharyngeal and tracheal secretions of children with respiratory syncytial virus disease.* Pediatr Infect Dis J, 1999. **18**(2): p. 115-22.
54. Haeberle, H.A., et al., *Inducible expression of inflammatory chemokines in respiratory syncytial virus-infected mice: role of MIP-1alpha in lung pathology.* J Virol, 2001. **75**(2): p. 878-90.
55. McNamara, P.S., et al., *Production of chemokines in the lungs of infants with severe respiratory syncytial virus bronchiolitis.* J Infect Dis, 2005. **191**(8): p. 1225-32.
56. McNamara, P.S., et al., *Bronchoalveolar lavage cellularity in infants with severe respiratory syncytial virus bronchiolitis.* Arch Dis Child, 2003. **88**(10): p. 922-6.

57. Abu-Harb, M., et al., *IL-8 and neutrophil elastase levels in the respiratory tract of infants with RSV bronchiolitis.* Eur Respir J, 1999. **14**(1): p. 139-43.

58. Garofalo, R., et al., *Eosinophil degranulation in the respiratory tract during naturally acquired respiratory syncytial virus infection.* J Pediatr, 1992. **120**(1): p. 28-32.

59. Peebles, R.S., Jr. and B.S. Graham, *Pathogenesis of respiratory syncytial virus infection in the murine model.* Proc Am Thorac Soc, 2005. **2**(2): p. 110-5.

60. De Weerd, W., W.N. Twilhaar, and J.L. Kimpen, *T cell subset analysis in peripheral blood of children with RSV bronchiolitis.* Scand J Infect Dis, 1998. **30**(1): p. 77-80.

61. Lo, M.S., R.M. Brazas, and M.J. Holtzman, *Respiratory syncytial virus nonstructural proteins NS1 and NS2 mediate inhibition of Stat2 expression and alpha/beta interferon responsiveness.* J Virol, 2005. **79**(14): p. 9315-9.

62. Swedan, S., A. Musiyenko, and S. Barik, *Respiratory syncytial virus nonstructural proteins decrease levels of multiple members of the cellular interferon pathways.* J Virol, 2009. **83**(19): p. 9682-93.

63. Durbin, J.E., et al., *The role of IFN in respiratory syncytial virus pathogenesis.* J Immunol, 2002. **168**(6): p. 2944-52.

64. Graham, B.S., et al., *Role of T lymphocyte subsets in the pathogenesis of primary infection and rechallenge with respiratory syncytial virus in mice.* J Clin Invest, 1991. **88**(3): p. 1026-33.

65. Fulton, R.B., D.K. Meyerholz, and S.M. Varga, *Foxp3+ CD4 regulatory T cells limit pulmonary immunopathology by modulating the CD8 T cell response during respiratory syncytial virus infection.* J Immunol, 2010. **185**(4): p. 2382-92.

66. Lee, D.C., et al., *CD25+ natural regulatory T cells are critical in limiting innate and adaptive immunity and resolving disease following respiratory syncytial virus infection.* J Virol, 2010. **84**(17): p. 8790-8.

67. Bem, R.A., J.B. Domachowske, and H.F. Rosenberg, *Animal models of human respiratory syncytial virus disease.* Am J Physiol Lung Cell Mol Physiol, 2011. **301**(2): p. L148-56.

68. Moore, M.L. and R.S. Peebles, Jr., *Respiratory syncytial virus disease mechanisms implicated by human, animal model, and in vitro data facilitate vaccine strategies and new therapeutics.* Pharmacol Ther, 2006. **112**(2): p. 405-24.
69. Byrd, L.G. and G.A. Prince, *Animal models of respiratory syncytial virus infection.* Clin Infect Dis, 1997. **25**(6): p. 1363-8.
70. Domachowske, J.B., C.A. Bonville, and H.F. Rosenberg, *Animal models for studying respiratory syncytial virus infection and its long term effects on lung function.* Pediatr Infect Dis J, 2004. **23**(11 Suppl): p. S228-34.
71. Dreizin, R.S., et al., *[Experimental RS virus infection of cotton rats. A viral and immunofluorescent study].* Vopr Virusol, 1971. **16**(6): p. 670-6.
72. Prince, G.A., et al., *Respiratory syncytial virus infection in inbred mice.* Infect Immun, 1979. **26**(2): p. 764-6.
73. Cormier, S.A., D. You, and S. Honnegowda, *The use of a neonatal mouse model to study respiratory syncytial virus infections.* Expert Rev Anti Infect Ther, 2010. **8**(12): p. 1371-80.
74. Easton, A.J., J.B. Domachowske, and H.F. Rosenberg, *Animal pneumoviruses: molecular genetics and pathogenesis.* Clin Microbiol Rev, 2004. **17**(2): p. 390-412.
75. Dyer, K.D., et al., *The Pneumonia Virus of Mice (PVM) model of acute respiratory infection.* Viruses, 2012. **4**(12): p. 3494-510.
76. Shrivastava, P., E. Watkiss, and S. van Drunen Littel-van den Hurk, *The response of aged mice to primary infection and re-infection with pneumonia virus of mice depends on their genetic background.* Immunobiology, 2016. **221**(3): p. 494-502.
77. Shrivastava, P., et al., *Blunted inflammatory and mucosal IgA responses to pneumonia virus of mice in C57BL/6 neonates are correlated to reduced protective immunity upon re-infection as elderly mice.* Virology, 2015. **485**: p. 233-43.
78. Paccaud, M.F. and C. Jacquier, *A respiratory syncytial virus of bovine origin.* Arch Gesamte Virusforsch, 1970. **30**(4): p. 327-42.

79. Stott, E.J. and G. Taylor, *Respiratory syncytial virus. Brief review.* Arch Virol, 1985. **84**(1-2): p. 1-52.
80. Valarcher, J.F. and G. Taylor, *Bovine respiratory syncytial virus infection.* Vet Res, 2007. **38**(2): p. 153-80.
81. Gershwin, L.J., et al., *Effect of infection with bovine respiratory syncytial virus on pulmonary clearance of an inhaled antigen in calves.* Am J Vet Res, 2008. **69**(3): p. 416-22.
82. Gershwin, L.J., et al., *Single Pathogen Challenge with Agents of the Bovine Respiratory Disease Complex.* PLoS One, 2015. **10**(11): p. e0142479.
83. Masihi, K.N., *Fighting infection using immunomodulatory agents.* Expert Opin Biol Ther, 2001. **1**(4): p. 641-53.
84. Hengel, H. and K.N. Masihi, *Combinatorial immunotherapies for infectious diseases.* Int Immunopharmacol, 2003. **3**(8): p. 1159-67.
85. Jantan, I., W. Ahmad, and S.N. Bukhari, *Plant-derived immunomodulators: an insight on their preclinical evaluation and clinical trials.* Front Plant Sci, 2015. **6**: p. 655.
86. Pirofski, L.A. and A. Casadevall, *Immunomodulators as an antimicrobial tool.* Curr Opin Microbiol, 2006. **9**(5): p. 489-95.
87. Masihi, K.N. and H. Schafer, *Overview of biologic response modifiers in infectious disease.* Infect Dis Clin North Am, 2011. **25**(4): p. 723-31.
88. Masihi, K.N., *Immunomodulatory agents for prophylaxis and therapy of infections.* Int J Antimicrob Agents, 2000. **14**(3): p. 181-91.
89. Mutwiri, G., et al., *Combination adjuvants: the next generation of adjuvants?* Expert Rev Vaccines, 2011. **10**(1): p. 95-107.
90. Vetvicka, V. and J. Vetvickova, *Natural immunomodulators and their stimulation of immune reaction: true or false?* Anticancer Res, 2014. **34**(5): p. 2275-82.
91. Lim, Y.T., *Vaccine adjuvant materials for cancer immunotherapy and control of infectious disease.* Clin Exp Vaccine Res, 2015. **4**(1): p. 54-8.
92. McKee, A.S., M.W. Munks, and P. Marrack, *How do adjuvants work? Important considerations for new generation adjuvants.* Immunity, 2007. **27**(5): p. 687-90.

93. Kapoor, R., V. Vijjan, and P. Singh, *Bacillus Calmette-Guerin in the management of superficial bladder cancer.* Indian J Urol, 2008. **24**(1): p. 72-6.
94. Schon, M.P. and M. Schon, *Imiquimod: mode of action.* Br J Dermatol, 2007. **157 Suppl 2**: p. 8-13.
95. Thotathil, Z. and M.B. Jameson, *Early experience with novel immunomodulators for cancer treatment.* Expert Opin Investig Drugs, 2007. **16**(9): p. 1391-403.
96. Kanzler, H., et al., *Therapeutic targeting of innate immunity with Toll-like receptor agonists and antagonists.* Nat Med, 2007. **13**(5): p. 552-9.
97. Antachopoulos, C. and E. Roilides, *Cytokines and fungal infections.* Br J Haematol, 2005. **129**(5): p. 583-96.
98. Zon, L.I., C. Arkin, and J.E. Groopman, *Haematologic manifestations of the human immune deficiency virus (HIV).* Br J Haematol, 1987. **66**(2): p. 251-6.
99. Hazel, D.L., A.C. Newland, and S.M. Kelsey, *Malignancy: Granulocyte Colony Stimulating Factor Increases the Efficacy of Conventional Amphotericin in the Treatment of Presumed Deep-Seated Fungal Infection in Neutropenic Patients following Intensive Chemotherapy or Bone Marrow Transplantation for Haematological Malignancies.* Hematology, 1999. **4**(4): p. 305-311.
100. Marshak-Rothstein, A., *Toll-like receptors in systemic autoimmune disease.* Nat Rev Immunol, 2006. **6**(11): p. 823-35.
101. Barrat, F.J., et al., *Treatment of lupus-prone mice with a dual inhibitor of TLR7 and TLR9 leads to reduction of autoantibody production and amelioration of disease symptoms.* Eur J Immunol, 2007. **37**(12): p. 3582-6.
102. Garg, R., et al., *Vaccination with the RSV fusion protein formulated with a combination adjuvant induces long-lasting protective immunity.* J Gen Virol, 2014. **95**(Pt 5): p. 1043-54.
103. Garg, R., et al., *Induction of mucosal immunity and protection by intranasal immunization with a respiratory syncytial virus subunit vaccine formulation.* J Gen Virol, 2014. **95**(Pt 2): p. 301-6.
104. Garg, R., et al., *The respiratory syncytial virus fusion protein formulated with a novel combination adjuvant induces balanced immune responses in lambs with maternal antibodies.* Vaccine, 2015. **33**(11): p. 1338-44.

105. Zhou, Z.X., B.C. Zhang, and L. Sun, *Poly(I:C) induces antiviral immune responses in Japanese flounder (Paralichthys olivaceus) that require TLR3 and MDA5 and is negatively regulated by Myd88.* PLoS One, 2014. **9**(11): p. e112918.

106. Huang, C.C., et al., *A pathway analysis of poly(I:C)-induced global gene expression change in human peripheral blood mononuclear cells.* Physiol Genomics, 2006. **26**(2): p. 125-33.

107. Martins, K.A., S. Bavari, and A.M. Salazar, *Vaccine adjuvant uses of poly-IC and derivatives.* Expert Rev Vaccines, 2015. **14**(3): p. 447-59.

108. Zhao, J., et al., *Intranasal treatment with poly(I*C) protects aged mice from lethal respiratory virus infections.* J Virol, 2012. **86**(21): p. 11416-24.

109. Tewari, K., et al., *Poly(I:C) is an effective adjuvant for antibody and multi-functional CD4+ T cell responses to Plasmodium falciparum circumsporozoite protein (CSP) and alphaDEC-CSP in non human primates.* Vaccine, 2010. **28**(45): p. 7256-66.

110. Nijnik, A., et al., *Synthetic cationic peptide IDR-1002 provides protection against bacterial infections through chemokine induction and enhanced leukocyte recruitment.* J Immunol, 2010. **184**(5): p. 2539-50.

111. Madera, L. and R.E. Hancock, *Synthetic immunomodulatory peptide IDR-1002 enhances monocyte migration and adhesion on fibronectin.* J Innate Immun, 2012. **4**(5-6): p. 553-68.

112. Wu, M. and R.E. Hancock, *Improved derivatives of bactenecin, a cyclic dodecameric antimicrobial cationic peptide.* Antimicrob Agents Chemother, 1999. **43**(5): p. 1274-6.

113. Hilchie, A.L., K. Wuerth, and R.E. Hancock, *Immune modulation by multifaceted cationic host defense (antimicrobial) peptides.* Nat Chem Biol, 2013. **9**(12): p. 761-8.

114. Lai, Y. and R.L. Gallo, *AMPed up immunity: how antimicrobial peptides have multiple roles in immune defense.* Trends Immunol, 2009. **30**(3): p. 131-41.

115. Mutwiri, G., et al., *Poly[di(sodium carboxylatoethylphenoxy)phosphazene] (PCEP) is a potent enhancer of mixed Th1/Th2 immune responses in mice immunized with influenza virus antigens.* Vaccine, 2007. **25**(7): p. 1204-13.

116. Andrianov, A.K., A. Marin, and J. Chen, *Synthesis, properties, and biological activity of poly[di(sodium carboxylatoethylphenoxy)phosphazene]*. Biomacromolecules, 2006. **7**(1): p. 394-9.

117. Awate, S., et al., *The adjuvant PCEP induces recruitment of myeloid and lymphoid cells at the injection site and draining lymph node.* Vaccine, 2014. **32**(21): p. 2420-7.

118. Kovacs-Nolan, J., et al., *CpG oligonucleotide, host defense peptide and polyphosphazene act synergistically, inducing long-lasting, balanced immune responses in cattle.* Vaccine, 2009. **27**(14): p. 2048-54.

119. Awate, S., et al., *Activation of adjuvant core response genes by the novel adjuvant PCEP.* Mol Immunol, 2012. **51**(3-4): p. 292-303.

120. Awate, S., et al., *Caspase-1 Dependent IL-1beta Secretion and Antigen-Specific T-Cell Activation by the Novel Adjuvant, PCEP.* Vaccines (Basel), 2014. **2**(3): p. 500-14.

121. Kovacs-Nolan, J., et al., *The novel adjuvant combination of CpG ODN, indolicidin and polyphosphazene induces potent antibody- and cell-mediated immune responses in mice.* Vaccine, 2009. **27**(14): p. 2055-64.

122. Onyeji, C.O., et al., *Influence of adjunctive interferon-gamma on treatment of gentamicin- and vancomycin-resistant Enterococcus faecalis infection in mice.* Int J Antimicrob Agents, 1999. **12**(4): p. 301-9.

123. Klinman, D.M., J. Conover, and C. Coban, *Repeated administration of synthetic oligodeoxynucleotides expressing CpG motifs provides long-term protection against bacterial infection.* Infect Immun, 1999. **67**(11): p. 5658-63.

124. Norton, E.B., et al., *Prophylactic administration of bacterially derived immunomodulators improves the outcome of influenza virus infection in a murine model.* J Virol, 2010. **84**(6): p. 2983-95.

125. Bonville, C.A., et al., *Altered pathogenesis of severe pneumovirus infection in response to combined antiviral and specific immunomodulatory agents.* J Virol, 2003. **77**(2): p. 1237-44.
126. Holt, P.G., et al., *Regulation of immunological homeostasis in the respiratory tract.* Nat Rev Immunol, 2008. **8**(2): p. 142-52.
127. Wissinger, E., J. Goulding, and T. Hussell, *Immune homeostasis in the respiratory tract and its impact on heterologous infection.* Semin Immunol, 2009. **21**(3): p. 147-55.
128. Tumpey, T.M., et al., *Pathogenicity of influenza viruses with genes from the 1918 pandemic virus: functional roles of alveolar macrophages and neutrophils in limiting virus replication and mortality in mice.* J Virol, 2005. **79**(23): p. 14933-44.
129. Kolli, D., et al., *Alveolar macrophages contribute to the pathogenesis of human metapneumovirus infection while protecting against respiratory syncytial virus infection.* Am J Respir Cell Mol Biol, 2014. **51**(4): p. 502-15.
130. Pribul, P.K., et al., *Alveolar macrophages are a major determinant of early responses to viral lung infection but do not influence subsequent disease development.* J Virol, 2008. **82**(9): p. 4441-8.
131. Gabelloni, M.L., et al., *Mechanisms regulating neutrophil survival and cell death.* Semin Immunopathol, 2013. **35**(4): p. 423-37.
132. Tate, M.D., A.G. Brooks, and P.C. Reading, *The role of neutrophils in the upper and lower respiratory tract during influenza virus infection of mice.* Respir Res, 2008. **9**: p. 57.
133. Drescher, B. and F. Bai, *Neutrophil in viral infections, friend or foe?* Virus Res, 2013. **171**(1): p. 1-7.
134. Bonville, C.A., et al., *Interferon-gamma coordinates CCL3-mediated neutrophil recruitment in vivo.* BMC Immunol, 2009. **10**: p. 14.
135. van Helden, M.J., et al., *Pre-existing virus-specific CD8(+) T-cells provide protection against pneumovirus-induced disease in mice.* Vaccine, 2012. **30**(45): p. 6382-8.

136. McNab, F., et al., *Type I interferons in infectious disease.* Nat Rev Immunol, 2015. **15**(2): p. 87-103.
137. Jin, B., et al., *Immunomodulatory effects of dsRNA and its potential as vaccine adjuvant.* J Biomed Biotechnol, 2010. **2010**: p. 690438.
138. Shi, C. and E.G. Pamer, *Monocyte recruitment during infection and inflammation.* Nat Rev Immunol, 2011. **11**(11): p. 762-74.